This is to certify that the

dissertation entitled

A finite element approximation of the flow in a toroidal tube.

presented by

Adel N. Boules

has been accepted towards fulfillment
of the requirements for

Ph.D. degree in Mathematics

CY Wang
Major professor

Date June 5, 87

A FINITE ELEMENT APPROXIMATION OF THE FLOW IN A TOROIDAL TUBE

By

Adel Boules

AN ABSTRACT OF A DISSERTATION

SUBMITTED TO

Michigan State University

in partial fulfillment of the requirements

for the degree of

DOCTOR OF PHILOSOPHY

Department of Mathematics

1987

ABSTRACT

A FINITE ELEMENT APPROXIMATION
OF THE FLOW IN A TOROIDAL TUBE

BY

ADEL BOULES

The problem is to compute the velocity field of an incompressible viscous fluid in a toroidal pipe under the effect of constant pressure gradient in the axial direction. The complete set of momentum and continuity equations were derived. The motion depends on two parameters: The Reynolds number and curvature ratio.

An appropriate function space was introduced, and a variational formulation of the problem in that space was defined.

A proof of existence and uniqueness of the solution was then presented.

Using a finite element approximation, the continuous infinite dimensional problem was replaced by a finite dimensional (yet nonlinear) approximate problem.

Two methods were used to solve the finite element equations:

(a) A direct linearization iterative scheme which was shown to converge to the solution of the approximate problem. This scheme has the rather serious drawback that at each iteration one must compute and solve a different set of unsymmetric linear equations.

(b) A least squares formulation was presented. In this formulation the solution of the problem is the minimizer of a certian "cost" functional. A conjugate gradient scheme was found most efficient in finding the minimizer of the cost functional and hence the solution to the problem.

The great advantage of this scheme is that during the different steps of the conjugate gradient scheme, one solves the same symmetric positive definite banded matrix equation for different forcing terms. Thus we need to compute and factor this constant matrix only once during the entire computation.

Being symmetric and banded, the matrix is easy to store compactly thus allowing the use of a fine mesh, and consequently producing greater accuracy. Because the matrix is also positive definite, it can be factored by the stable Choleski decomposition.

Both schemes were implemented and the velocity field was computed. The two schemes produced almost identical results for all cases computed. Excellent agreement is also achieved in comparison with the results of previous investigators.

A perturbation solution of the equations of motion was then obtained for small curvature ratios and low Reynolds numbers. These solutions also compare well with the numerical solutions described above.

ACKNOWLEDGEMENTS

I would like to express my gratitude to Professor C.- Y. Wang, my thesis advisor, for his patience and guidance during the course of this work. I also wish to extend my thanks to the members of my thesis committee, Professors D. Yen, J. Kurtz, B. Drachman and C. MacCluer.

I should also acknowledge my gratitude to Mrs. B. Reiter, the mathematics librarian, for her kind assistance, and to Miss S. Polomsky for typing this dissertation.

Finally, I wish to express my sincerest thanks to the Case center for Computer Aided Engineering, for furnishing the computer equipment without which this work would not have been possible.

DEDICATED TO

MY WIFE AND MY SON

TABLE OF CONTENTS

LIST OF FIGURES

LIST OF TABLES

CHAPTER 1: INTRODUCTION AND FORMULATION

1.1 Description of the problem

This work is concerned with the flow of an incompressible viscous fluid in a toroidal pipe. Duct flows are important in many engineering and biological applications, such as piping systems, the design of heat exchangers, and the study of blood flow in arterial systems. The geometry and coordinate system are shown in Figure 1, where O is the center of the torus, and C is the center of the circular cross section. Let one of the independent variables be the arc length X^3 of the center line of the pipe measured from a fixed point F, and Let T, N, B be unit vectors along the tangent, normal and binormal of the center line, thus N and B lie in the plane of the cross section, and for a typical point Q in that plane we have

$$Q = X^1 N + X^2 B$$

The flow is assumed to be laminar, steady, fully developed, and driven by a constant pressure gradient in the axial direction. We therefore assume that the pressure P is a linear function of X^3, and that the velocity components are functions of X^1 and X^2 only.

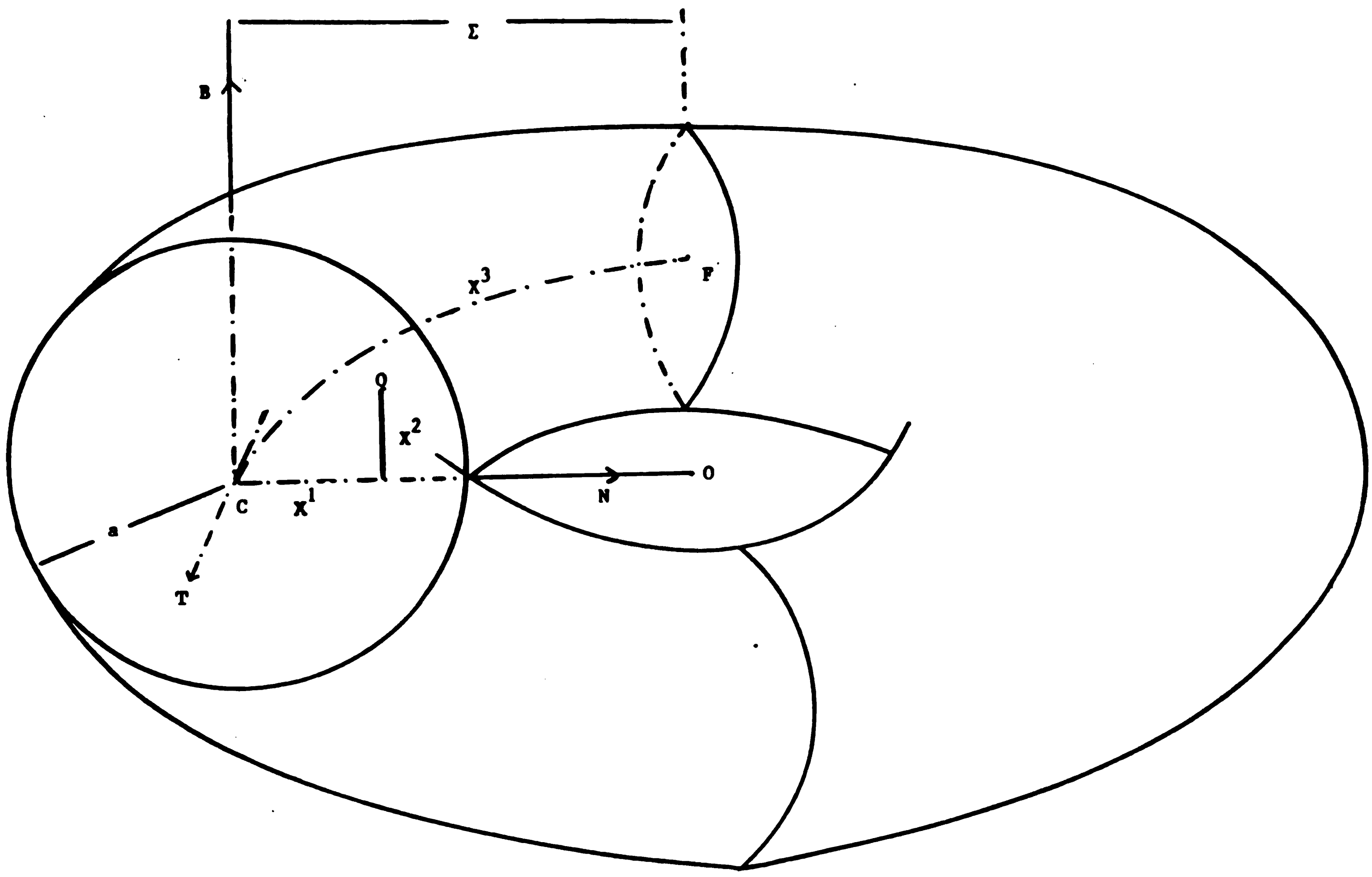

Geometry and coordinate system

Figure 1

1.2 Governing equations

The major portion of this work is concerned with a circular cross section. Let Σ be the radius of the torus, a be the radius of the cross section, and let $\kappa = \frac{1}{\Sigma}$ be the curvature of the tube. As was done in Wang (1981), we computed the metric tensors (g_{ij}) and (g^{ij}), and the Christoffel symbols Γ^i_{jk}. For a torus the system is orthogonal. The metric tensors are

$$(g_{ij}) = \begin{bmatrix} 1 & 0 & 0 \\ 0 & 1 & 0 \\ 0 & 0 & J \end{bmatrix}, \quad (g^{ij}) = \begin{bmatrix} 1 & 0 & 0 \\ 0 & 1 & 0 \\ 0 & 0 & 1/J \end{bmatrix} = (g_{ij})^{-1}$$

where
$$J = (1 - \kappa X^1)^2$$

There are only two non-zero Christoffel symbols

$$\Gamma^3_{13} = -\frac{\kappa}{\sqrt{J}}, \quad \Gamma^1_{33} = \kappa\sqrt{J}$$

For $j = 1, 2, 3$, let U^j be the velocity component in the X^j direction and let V^j be the tensorial components in the same directions, thus $V^1 = U^1$, $V^2 = U^2$, $V^3 = U^3 / \sqrt{J}$. The covariant velocity derivatives are given by

$$V^i_{,jk} = \frac{\partial^2 V^i}{\partial X^k \partial X^j} + \frac{\partial}{\partial X^k}(\Gamma^i_{\alpha j} V^\alpha) - \Gamma^\alpha_{jk}\left(\frac{\partial V^i}{\partial X^\alpha} + \Gamma^i_{\alpha\beta} V^\beta\right) + \Gamma^i_{\alpha k}\left(\frac{\partial V^\alpha}{\partial X^j} + \Gamma^\alpha_{j\beta} V^\beta\right)$$

where summation over repeated indices is understood.

A list of the velocity derivatives $V^i_{,jk}$ is given in appendix A. We now substitute the above in the tensorial form of the Navier-Stokes equations:

$$V^j\left(\frac{\partial V^i}{\partial X^j} + \Gamma^i_{\alpha j}V^\alpha\right) = -\frac{g^{ij}}{\rho}\frac{\partial P}{\partial X^j} + \nu g^{kj}V^i_{,jk}, \qquad i = 1,\ 2,\ 3,$$

$$\frac{\partial V^i}{\partial X^i} + \Gamma^i_{\alpha i}V^\alpha = 0$$

Where ρ is the density, and ν is the coefficient of kinematic viscousity both assumed constant. After some rearrangement, the momentum equations can be written as

$$(1.1)\quad \sqrt{J}\left(U^1\frac{\partial}{\partial X^1} + U^2\frac{\partial}{\partial X^2}\right) U^1 + \kappa(U^3)^2 = -\frac{\sqrt{J}}{\rho}\frac{\partial P}{\partial X^1} + \nu\ \mathrm{div}\ (\sqrt{J}\nabla U^1) - \frac{\kappa^2}{\sqrt{J}}U^1$$

$$(1.2)\quad \sqrt{J}\left(U^1\frac{\partial}{\partial X^1} + U^2\frac{\partial}{\partial X^2}\right) U^2 = -\frac{\sqrt{J}}{\rho}\frac{\partial P}{\partial X^2} + \nu\ \mathrm{div}(\sqrt{J}\ \nabla U^2)$$

$$(1.3)\quad \sqrt{J}\left(U^1\frac{\partial}{\partial X^1} + U^2\frac{\partial}{\partial X^2}\right)U^3 - \kappa\ U^1U^3 = -\frac{1}{\rho}\frac{\partial P}{\partial X^3} + \nu\ \mathrm{div}(\sqrt{J}\ \nabla U^3) - \frac{\kappa^2}{\sqrt{J}}U^3$$

and the continuity equation

$$(1.4)\qquad \frac{\partial}{\partial X^1}(\sqrt{J}U^1) + \frac{\partial}{\partial X^2}(\sqrt{J}U^2) = 0$$

where for a scalar function $\varphi(X^1,\ X^2)$

$$\nabla\varphi = \frac{\partial\varphi}{\partial X^1}\mathbf{N} + \frac{\partial\varphi}{\partial X^2}\mathbf{B}$$

and for a vector function $\Phi = (\varphi^1, \varphi^2, \varphi^3)$

$$\operatorname{div} \Phi = \frac{\partial \varphi^1}{\partial X^1} + \frac{\partial \varphi^2}{\partial X^2} \qquad (\varphi^i = \varphi^i(X^1, X^2))$$

Thus the gradient ∇ and the divergence div, and later the Laplacian are all two dimensional operators. This convention will be adopted throughout the thesis to simplify notation.

We normalize the independent and dependent variables as follows:

$$X^j = ax_j, \ U^j = \frac{\nu}{a} u_j, \ P = \frac{\rho\nu^2}{a^2} p$$

Substituting in equations (1.1) - (1.4) yields the dimensionless momentum and continuity equations

$$(1.5) \quad \sqrt{J}\left(u_1\frac{\partial}{\partial x_1} + u_2\frac{\partial}{\partial x_2}\right)u_1 + \epsilon u_3^2 = -\sqrt{J}\,\frac{\partial p}{\partial x_1} + \operatorname{div}(\sqrt{J}\nabla u_1) - \frac{\epsilon^2}{\sqrt{J}}\,u_1$$

$$(1.6) \quad \sqrt{J}\left(u_1\frac{\partial}{\partial x_1} + u_2\frac{\partial}{\partial x_2}\right)u_2 = -\sqrt{J}\,\frac{\partial p}{\partial x_2} + \operatorname{div}(\sqrt{J}\nabla u_2)$$

$$(1.7) \quad \sqrt{J}\left(u_1\frac{\partial}{\partial x_1} + u_2\frac{\partial}{\partial x_2}\right)u_3 - \epsilon u_1 u_3 = 4R + \operatorname{div}(\sqrt{J}\nabla u_3) - \frac{\epsilon^2}{\sqrt{J}}\,u_3$$

$$(1.8) \qquad \operatorname{div}(\sqrt{J}u) = 0$$

where $R = \dfrac{-a^3}{4\rho\nu^2}\dfrac{\partial P}{\partial X^3}$ is the Reynolds' number.

$\epsilon = a/\Sigma$ is the curvature ratio, and now $\sqrt{J} = 1 - \epsilon x_1$.

Equations (1.5) - (1.8) are solved subject to the boundary conditions

$$(1.9) \qquad u_j\Big|_{\Gamma} = 0 \qquad j = 1, 2, 3,$$

where Γ is the boundary of the unit disk

$$\Omega = \{x_1^2 + x_2^2 < 1\}$$

Note that when $\epsilon = 0$, equations (1.5) - (1.9) reduce to the equations describing the motion in a straight pipe.

The velocity component u_3 will henceforth be called the axial velocity (or primary flow), and the transversal velocities u_1, u_2 will be referred to as the secondary flow. Most of this work is devoted to investigating efficient approximations of equations (1.5) - (1.9).

1.3 Literature review

In this section we give a brief account of some studies related to our work. An extensive compilation of references can be found in the review by Berger, Talbot, and Yao (1983).

We begin by giving an equivalent set of equations to (1.5) - (1.7) which uses the Dean number $D = 4R\sqrt{2\epsilon}$, and the curvature ratio ϵ as the governing parameters. If in equation (1.5) - (1.7) we substitute $u_3 = \dfrac{u_3'}{\sqrt{2\epsilon}}$ and drop the prime, we obtain the following set of equations.

$$(1.10) \quad \sqrt{J}(u_1\frac{\partial}{\partial x_1} + u_2 \frac{\partial}{\partial x_2})\, u_1 + \frac{1}{2} u_3^2 = - \sqrt{J}\, \frac{\partial p}{\partial x_1} + \mathrm{div}(\sqrt{J}\nu u_1) - \frac{\epsilon^2}{\sqrt{J}} u_1$$

$$(1.11)\quad \sqrt{J}(u_1\frac{\partial}{\partial x_1} + u_2\frac{\partial}{\partial x_2})\, u_2 \qquad = -\sqrt{J}\frac{\partial p}{\partial x_2} + \operatorname{div}(\sqrt{J}\nabla u_2)$$

$$(1.12)\quad \sqrt{J}(u_1\frac{\partial}{\partial x_1} + u_2\frac{\partial}{\partial x_2})\, u_3 - \epsilon u_1 u_3 = D + \operatorname{div}\,(\sqrt{J}\,\nabla u_3) - \frac{\epsilon^2}{\sqrt{J}}\, u_3$$

$$(1.13)\qquad \operatorname{div}(u\sqrt{J}) = 0$$

where $D = 4R\sqrt{2\epsilon}$ is the Dean number as defined by McConalogue and Srivastava (1968). Clearly equations (1.10) - (1.13) are completely equivalent to equation (1.5) - (1.8) except for renaming the parameters and rescaling the axial velocity u_3.

Now if we set $\epsilon = 0$ in equations (1.10) - (1.13) we obtain a commonly used set of approximate equations describing the motion in "the limit of zero curvature".

$$(1.14)\qquad (u_1\frac{\partial}{\partial x_1} + u_2\frac{\partial}{\partial x_2})\, u_1 + \frac{1}{2}u_3^2 = -\frac{\partial p}{\partial x_1} + \Delta u_1$$

$$(1.15)\qquad (u_1\frac{\partial}{\partial x_1} + u_2\frac{\partial}{\partial x_2})\, u_2 \qquad = -\frac{\partial p}{\partial x_2} + \Delta u_2$$

$$(1.16)\qquad (u_1\frac{\partial}{\partial x_1} + u_2\frac{\partial}{\partial x_2})\, u_3 \qquad = D + \Delta u_3$$

$$(1.17)\qquad \operatorname{div} u = 0$$

where $\Delta = \frac{\partial^2}{\partial x_1^2} + \frac{\partial^2}{\partial x_2^2}$ is the 2 dimensional Laplacian.

Equations (1.14) - (1.17) will henceforth be referred to as Dean's equations for the motion in the limit of zero curvature. The same equations can be seen to be equivalent to the equations used by McConalogue and Srivastava (1968), Greenspan (1973), Collins and Dennis (1975), Dennis and Ng (1982) and Dennis (1980), except that the authors of these works employed a polar coordinate system in the plane of the cross section, and used a vorticity-stream function-axial velocity formulation. The authors of the papers cited above used a variety of numerical methods to solve Dean's equations, and among them Collins and Dennis (1975) seem to have achieved the most accurate set of results covering the range $96 \leq D \leq 5000$. The accuracy of their calculation was later confirmed by the study of Dennis (1980) and that of Dennis and Ng (1982).

Collins and Dennis (1975) also report very good agreement with experimental results and results obtained by applying boundary layer methods which they documented in their paper.

We believe that there is enough evidence of the reliability of the results of Collins and Dennis (1975), and therefore take their results as a reference set of solutions against which we measure the accuracy of our solutions. It should be noted that all the references mentioned above deal with the flow in the limit of zero curvature, and that none of them addresses the effect of curvature on the flow.

There are a few works that attempt to study the effect of curvature. Truesdell and Adler (1970) used a finite difference method to obtain solutions up to $D = 3578$ and $\epsilon = .1$, with a set of equations first derived by Cuming (1952). The equations used by Truesdell and Adler (1970) can be manipulated into equations (1.5) - (1.8) of this work. The results of Truesdell and Adler (1970) however were not sufficiently accurate beyond $D = 1131$, as the authors of that work noted in their paper. Most of the works mentioned above used finite difference methods which often requires a great number of mesh points to achieve reasonable accuracy, which in turn puts tremendous bearing on computer memory and execution time (Collins and Dennis (1975) used a finite difference mesh with 2921 points and achieved the same accuracy we did in this work with a finite element mesh of 489 nodes). Many of the above authors also used a vorticity - stream function - axial velocity formulation, and were confronted with the difficulty of approximating the axial vorticity at the boundary of the region. Finite difference approximations also suffer the further difficulty that for different cross sections, different formulations of the problem must be used. For example, Collins and Dennis (1975) used a polar mesh for a circular cross section and were forced to use the equations of motion in polar coordinates, and later Collins and Dennis (1976) had to convert the equations to rectangular form in order to solve the flow problem in a triangular duct.

The switching of formulation often requires substantial modifications of numerical techniques and computer code. We view the problem of duct flow as essentially one problem regardless of the shape of the cross section, and consequently believe that a unified approach is needed to avoid redundency. The situation becomes worse if one uses a mesh that does not conform to the shape of the boundary. An example of this is the work of Truesdell and Adler (1970) who used a rectangular finite difference mesh to compute the flow in tubes of circular and elliptic cross sections, and there they used a number of fictitious boundary points to avoid the difficulty of approximating derivatives near the boundary. Works on duct flows in cross sections other than the circle include Cuming (1952), Truesdell and Adler

(1970), Joseph, Smith and Adler (1975), Collins and Dennis (1976).

1.4 Objectives and Organization

Our first goal in this work is to give an accurate mathematical description of the problem. In chapter 2 we introduce appropriate solution spaces and give an accurate variational formulation of equations (1.5) - (1.8). We then consider the questions of existence and uniqueness of the solution. The main objective of this work is to build efficient numerical schemes to solve equations (1.5) - (1.8), and since we believe that finite difference methods are rather cumbersome and expensive for the reasons stated in section 1.3, we utilize finite element methods to achieve our goal. Our solution method avoids all the problems classically associated with finite difference methods, and we believe it is far more efficient than methods used by earlier investigators.

In Chapter 3 we describe a finite element scheme to reduce the infinite dimensional problem to a finite dimensional nonlinear problem whose solutions are described in Chapters 3 and 5, and there we also give some details on the practical implementation of those schemes, which we hope will cast some light on the advantages of finite element approximations, and hence the computational efficiency of our solution. In chapter 4 we present our error analysis, and give a bound on $||u - u_h||$, where u is the exact solution, u_h is the approximate solution, and $|| \cdot ||$ denotes the norm in $H^1(\Omega)^3$

Numerical results and the physical discussion are given in Chapter 6. In Chapter 7, we apply a perturbation method to obtain solutions for the flow in a tube of elliptic cross section, and use our scheme to generate a numerical solution of the same problem. This was done for two reasons. On the one hand, it supplies further evidence that our computation is accurate, and on the other hand it demonstrates the ease with which finite elements are able to handle irregular boundaries. In particular the same scheme and the same computer program can be used to solve the problem for any shape of the cross section at the small additional expense of generating a finite element mesh to discretise the cross section.

From the physical point of view, it is our aim to show the effect of curvature on the velocity field, and to show the significant deviation of our solutions from those obtained in the limit of zero curvature.

We also study the effect of curvature on the flow rate, and discuss the adequacy of each of the parameters R and D to describe the motion.

CHAPTER 2: EXISTENCE AND UNIQUENESS

2.1 Preliminaries and notation

In this chapter we use standard functional analytic notations. For example if H is a Hilbert space, we denote the inner product by $(.,.)$, and distinguish the duality bracket between H and H^* by the superscripted bracket $(.,.)^*$, thus for $x \in H$ and $f \in H^*$, $(f,x)^* = f(x)$. The reason for this is that we do not always identify a Hilbert space with its dual in the canonical way via the Riesz-Fisher theorem. Throughout the chapter, Ω is the open unit disk, and all integrals are taken over Ω. We also use standard notations like $C_0^\infty(\Omega)$ for C^∞ functions of compact support in Ω, and $H_0^1(\Omega)$ for real valued functions on Ω which vanish in the sense of trace on the boundary of Ω, and whose generalized derivatives are also in $L^2(\Omega)$, with norm defined by

$$||u||^2 = ||u||_0^2 + ||\frac{\partial u}{\partial x_1}||_0^2 + ||\frac{\partial u}{\partial x_2}||_0^2 \quad \text{for } u \in H_0^1(\Omega)$$

where $||\cdot||_0$ denotes the usual norm on $L^2(\Omega)$. $||\cdot||_p$ will be used for the norm in $L^p(\Omega)$, and to distinguish the norm on $H_0^1(\Omega)$, we simply denote the norm on the latter space by $||\cdot||$. We also use standard notations like $C_0^\infty(\Omega)^3$ to denote the space $C_0^\infty(\Omega) \times C_0^\infty(\Omega) \times C_0^\infty(\Omega)$ and similarly for $H_0^1(\Omega)^2$, $H_0^1(\Omega)^3$ etc. Product spaces are given the product norm. Thus for $\mathbf{u} = (u_1, u_2, u_3) \in H_0^1(\Omega)^3$ (vector functions will be denoted by boldface letters)

$$||\mathbf{u}||^2 = \sum_{i=1}^{3} ||u_i||^2$$

The continuity equation

$$\operatorname{div}(u\sqrt{J}) = \frac{\partial(u_1\sqrt{J})}{\partial x_1} + \frac{\partial(u_2\sqrt{J})}{\partial x_2} = 0$$

suggests the introduction of the following space in which the above equation is automatically satisfied.

Difinition 2.1.1:

For $0 \leq \epsilon < 1$, define

$$V_\epsilon = \{u \in H_0^1(\Omega)^2 : \operatorname{div}\ (u\sqrt{J}) = 0\} \subsetneq H_0^1(\Omega)^2$$

Observe that $V_0 = \{u \in H_0^1(\Omega)^2 : \operatorname{div}\ u = 0\}$ is the space of divergence-free vector fields which has been studied in detail in Temam (1984) and Girault and Raviart (1979). Note that V_ϵ is the kernel of the linear operator $L_\epsilon : H_0^1(\Omega)^2 \to L^2(\Omega)$ defined by $L_\epsilon u = \operatorname{div}(u\sqrt{J})$. Note also that L_ϵ is the composition $\operatorname{div} \circ M_\epsilon$ where div is the divergence operator and $M_\epsilon : H_0^1(\Omega)^2 \to H_0^1(\Omega)^2$ is the multiplication operator defined by

$$M_\epsilon u = u\sqrt{J}$$

Lemma 2.1.1:

V_ϵ is a closed subspace of $H_0^1(\Omega)^2$. Thus V_ϵ is a Hilbert space with the norm $||\cdot||$.

Proof: Observe the the divergence operator is continuous, and that M_ϵ is a linear homeomorphism on $H_0^1(\Omega)^2$ since $\sqrt{J}$, $\frac{1}{\sqrt{J}} \in C^\infty(\Omega)$. Thus L_ϵ is bounded and $V_\epsilon = \text{Ker } L_\epsilon$ □

Definition 2.1.2:

$$L_0^2(\Omega) = \{p \in L^2(\Omega): \int p dx = 0\}$$

Lemma 2.1.2:

The linear operator L_ϵ defined before lemma 2.1.1 maps $H_0^1(\Omega)^2$ onto $L_0^2(\Omega)$.

Proof: Clearly for $u \in H_0^1(\Omega)^2$ we have

$$\int \text{div}(u\sqrt{J})dx = - \int_\Gamma \sqrt{J}\, u.n\, ds = 0,$$

since $u \in H_0^1(\Omega)^2$. Thus L_ϵ maps $H_0^1(\Omega)^2$ into $L_0^2(\Omega)$.

By theorem 3.5 page 32 of Girault and Raviart (1979), the divergence operator maps $H_0^1(\Omega)^2$ onto $L_0^2(\Omega)$. Hence given $q \in L_0^2(\Omega)$, there exists $v \in H_0^1(\Omega)^2$ such that div $v = q$. Set $u = v/\sqrt{J}$. Clearly $L_\epsilon u = q$ □

Lemma 2.1.3:

$$V_\epsilon \cap C_0^\infty(\Omega)^2 \text{ is dense in } V_\epsilon.$$

Proof: By theorem 3.8 page 36 of Girault and Raviart (1979).

$V_0 \cap C_0^\infty(\Omega)^2$ is dense in V_0. The result now follows directly since M_ϵ is a linear hemeomorphism on $H_0^1(\Omega)^2$. □

We now define the velocity solution space:

Definition 2.1.3:

$$X = V_\epsilon \times H_0^1(\Omega)$$

Observe that the continuity equation (1.8) does not involve the third velocity component u_3 and thus X is the natural space for a solution u of equations (1.5) - (1.8) to exist.

Since X is given the product norm, and $C_0^\infty(\Omega)$ is dense in $H_0^1(\Omega)$, the following lemma follows directly from lemmas 2.1.1 - 2.1.3.

Lemma 2.1.4:

(a) X is a closed subspace of $H_0^1(\Omega)^3$, and is therefore a Hilbert space

(b) The operator L_ϵ maps $H_0^1(\Omega)^3$ onto $L_0^2(\Omega)$, and $X = \ker L_\epsilon$.

(c) $X \cap C_0^\infty(\Omega)^3$ is dense in X. □

Remark: The two dimensional operator L_ϵ is extended in the obvious way

$$L_\epsilon u = \frac{\partial(u_1\sqrt{J})}{\partial x_1} + \frac{\partial(u_2\sqrt{J})}{\partial x_2}\ ; \qquad u = (u_1, u_2, u_3) \in H_0^1(\Omega)^3$$

2.2: Variational Formulation of the Problem

To motivate the variational definition of the problem, let us assume that smooth solutions (u,p) exist for equations (1.5) - (1.8). Multiplying equations (1.5) - (1.7) respectively by $w_1, w_2, w_3 \in H_0^1(\Omega)$, integrating over Ω, we obtain the following equation after integrating the viscous terms by parts and adding the resulting equations.

$$\int \nabla u \cdot \nabla w\sqrt{J}\, dx + \epsilon^2 \int \frac{1}{\sqrt{J}}(u_1 w_1 + u_3 w_3)\, dx + \sum_{j=1}^{3} \int\sqrt{J}\, w_j(u_1\frac{\partial}{\partial x_1} + u_2\frac{\partial}{\partial x_2})\, u_j dx$$
$$+ \epsilon \int (u_3 u_3 w_1 - u_1 u_3 w_3)dx = - \int\nabla p \cdot w\sqrt{J}\, dx + \int F \cdot w\, dx$$

where $u = (u_1, u_2, u_3)$, $w = (w_1, w_2, w_3)$, $F = \begin{bmatrix} 0 \\ 0 \\ 4R \end{bmatrix}$, and

$$F \cdot w = \sum_{j=1}^{3} F_j w_j = 4Rw_3.$$

The above equation can be written more compactly in the form

$$a_0(u,w) + B(u, u, w) = - (\nabla p, w\sqrt{J})_0 + (F, w)_0$$

where $(\cdot,\cdot)_o$ denotes the inner product in $L^2(\Omega)^3$, $\nabla u.\ \nabla w = \sum_{i=1}^{3} \nabla u_i \cdot \nabla w_i$ and

(2.1) $$a_o(u, w) = \int\nabla u \cdot \nabla w\, \sqrt{J}\, dx + \epsilon^2 \int \frac{1}{\sqrt{J}} (u_1 w_1 + u_3 w_3)dx$$

(2.2) $$B(u,v,w) = \sum_{j=1}^{3} \int \sqrt{J} w_j(u_1 \frac{\partial}{\partial x_1} + u_2 \frac{\partial}{\partial x_2})v_j dx + \epsilon\int(u_3 v_3 w_1 - u_1 v_3 w_3)dx$$

We now define the variational form of equations (1.5) - (1.8) and refer to the problem by (P).

(P) Find $u \in X$ and $p \in L_0^2(\Omega)$ such that

$$a_o(u,w) + B(u,u,w) = - (\nabla p,\ w\sqrt{J})^* + (F,w)^* \quad \text{for every } w \in H_0^1(\Omega)^3.$$

In the above, $(\nabla p,\ w\sqrt{J})^*$ is the duality bracket between $H_0^{-1}(\Omega)^3$ and $H_0^1(\Omega)^3$, thus ∇p is viewed as a bounded functional on $H_0^1(\Omega)^3$ defined by $(\nabla p,\ w\sqrt{J})^* = - \int p \operatorname{div} (w\sqrt{J})\, dx$. For the rest of this chapter $F \in H_0^{-1}(\Omega)^3$.

Proposition 2.2.1:

a_o is continuous, symmetric, bilinear, and coercive on $H_0^1(\Omega)^3$. Thus there exists a constant $\alpha > 0$ such that

$$a_o(u,u) \geq \alpha\ ||u||^2 \tag{2.3}$$

Proof: The result follows immediately from the Poincare inequality and the properties of $\sqrt{J}$ □

Proposition 2.2.2:

B is well defined, trilinear and separately continuous on $H_0^1(\Omega)^3$. Thus the number $\beta > 0$ defined by

$$\beta = \sup \left\{ \frac{|B(u,v,w)|}{||u||\ ||v||\ ||w||} :\ u,\ v,\ w \in H_0^1(\Omega)^3 \right\} \tag{2.4}$$

is finite.

Proof: The trilinearity of B is obvious once we prove that all the integrals appearing in the definition of B are finite.

Some of the integrals defining B have the form

$$\int \sqrt{J}\, w_j u_i \frac{\partial v_j}{\partial x_i} dx \quad (1 \le i \le 2,\ 1 \le j \le 3) \quad \text{where } u_i,\ v_j,\ w_j \in H_0^1(\Omega)$$

By the Sobolev imbedding theorem, $H_0^1(\Omega)$ is continuously imbedded in $L^4(\Omega)$, thus u_i, $w_j \in L^4(\Omega)$, and $||u_i||_4 \le C\ ||u_i||$, $||w_j||_4 \le C||w_j||$, and since $\frac{\partial v_j}{\partial x_i} \in L^2(\Omega)$, the generalized Holder inequality guarantees the finiteness of the above integrals, and together with the imbedding theorem and the boundedness of $\sqrt{J}$ gives

$$\int |\sqrt{J}\, w_j u_i \frac{\partial v_j}{\partial x_i}|\, dx \le C\ ||w_j||_4\ ||u_i||_4\ ||\frac{\partial v_j}{\partial x_i}||_0 \le C\ ||w_j||\ ||u_i||\ ||v_j||$$
$$\le C\ ||u||\ ||v||\ ||w||.$$

In the above, the symbol C denotes different positive constants. The other integrals involved in the definition of B have the form $\int u_i v_j w_k dx$. Using a similar argument, one can show that

$$\int |u_i v_j w_k| dx \le C\ ||u||\ ||v||\ ||w||.$$

The above inequalities imply that $|B(u,\ v,\ w)| \le C\ ||u||\ ||v||\ ||w||$ and the proof is complete. □

Now that we know that problem (P) is well defined, we give an equivalent form of the problem. Consider the following problem

(Q) Find $u \in X$ such that

$$a_0(u,w) + B(u,\ u,\ w) = (F,\ w)^* \text{ for every } w \in X$$

Clearly if (u,p) is a solution of problem (P), then u is also a solution of problem (Q) since div $(u\sqrt{J}) = 0$.

We now prove that the two problems are equivalent in the sense of the following proposition.

Proposition 2.2.3:

Suppose $u \in X$ is a solution of problem (Q). Then there exists a unique function $p \in L_0^2(\Omega)$ such that the pair (u,p) is a solution of problem (P).

Proof: Let us view L_ϵ as bounded linear operator from $H_0^1(\Omega)^3$ to $L_0^2(\Omega)^*$, where $L_0^2(\Omega)^*$ is the dual of $L_0^2(\Omega)$ and the two spaces are identified via the Riesz-Fischer theorem. Thus L_ϵ: $H_0^1(\Omega)^3 \to L_0^2(\Omega)^*$ is defined by

$$(L_\epsilon u,q)^* = \int qL_\epsilon u\, dx = \int q\, \mathrm{div}(u\sqrt{J})dx,\ q \in L_0^2(\Omega)$$

By lemma 2.1.4., L_ϵ maps $H_0^1(\Omega)^3$ onto $L_0^2(\Omega)^*$, thus the range of L_ϵ is closed, hence

$$\text{(2.5)} \qquad \mathrm{Range}\ (L_\epsilon^*) = (\ker L_\epsilon)^+ = X^+$$

where L_ϵ^*: $L_0^2(\Omega) \to (H_0^1(\Omega)^3)^* = H_0^{-1}(\Omega)^3$ is the adjoint of L_ϵ and X^+ is the annihilator of X defined by $X^+ = \{\ell \in H_0^{-1}(\Omega)^3\colon \ell(X) = 0\}$. Observe that by definition

$$(L_\epsilon^* q,\ u)^* = (L_\epsilon u,q)^* = \int q\, \mathrm{div}(u\sqrt{J})dx = -\ (\nabla q, u\sqrt{J})^*\ q \in L_0^2(\Omega), u \in H_0^1(\Omega)^3$$

Now assume that $u \in X$ is a solution of (Q). Define an element

$$\ell \in H_0^{-1}(\Omega)^3 \text{ by } \ell(w) = a_0(u,w) + B(u,u,w) - (F,w)^*, \; w \in H_0^1(\Omega)^3.$$

By assumption $\ell(w) = 0$ for $w \in X$, thus $\ell \in X^+$ and by (2.5) $\ell \in \text{Range } (L_\epsilon^*)$.

Thus there exists $p \in L_0^2(\Omega)$ such that $\ell = L_\epsilon^* p$ i.e.

$$a_0(u,w) + B(u,u,w) - (F,w)^* = (L_\epsilon^* p,w)^* = -(\nabla p, w\sqrt{J})^*$$

for every $w \in H_0^1(\Omega)^3$.

We have proved the existence of the function p promised in the statement. The uniqueness of p follows from the fact that L_ϵ maps $H_0^1(\Omega)^3$ onto $L_0^2(\Omega)$. $\square$

2.3: Existence

In this section, we prove that problem (Q) has a solution. Uniqueness is discussed in the next section. First we need the following properties of B.

Proposition 2.3.1:

(a) $B(u,u,u) = 0$ for every $u \in X$.

(b) $B(u,u,v) + B(v,v,u) = B(u-v,u-v,v)$ for every $u \in X$, $v \in X$.

Proof: Assume first that $u \in X \cap C_0^\infty(\Omega)^3$. In this case we have

$$B(u,u,u) = \sum_{j=1}^{3} \int \sqrt{J} u_j \left(u_1 \frac{\partial}{\partial x_1} + u_2 \frac{\partial}{\partial x_2}\right) u_j dx =$$

$$\frac{1}{2}\sum_{j=1}^{3}\int(\sqrt{J}u_1\frac{\partial}{\partial x_1} + \sqrt{J}u_2\frac{\partial}{\partial x_2})(u_j^2)dx = -\frac{1}{2}\sum_{j=1}^{3}\int u_j^2\,\mathrm{div}(u\sqrt{J})dx = 0$$

Now for $u \in X$, choose a sequence $u^n \in X \cap C_0^\infty(\Omega)^3$ such that $u^n \to u$ in X. This is possible by lemma 2.1.4. The trilinearity of B yields the identity

$$B(u-u^n,\ u-u^n,\ u-u^n) = B(u,u,u) - B(u^n,\ u^n,\ u^n) + B(u,\ u^n-u,\ u^n) + B(u^n-u,\ u^n,u) + B(u^n,\ u,\ u^n-u)$$

If in the above identity we let $n \to \infty$, use the fact that $B(u^n,u^n,u^n) = 0$ and the separate continuity of B (proposition 2.2.2), we obtain $B(u,u,u) = 0$ which proves (a). The proof of (b) is trivial.

Definition 2.3.1:

We define the auxilliary trilinear form

$$B_1(u,v,w) = \sum_{j=1}^{3}\int \sqrt{J}w_j(u_1\frac{\partial}{\partial x_1} + u_2\frac{\partial}{\partial x_2})v_j dx \tag{2.6}$$

Observe that

$$B(u,v,w) = B_1(u,v,w) + \epsilon \int(u_3v_3w_1 - u_1v_3w_3)dx \tag{2.7}$$

The proof of the following proposition is similar to that of proposition 2.3.1 and is therefore omitted.

Proposition 2.3.2:

For $u,\ v,\ w \in X$

(a) $B_1(u,v,v) = 0$

(b) $B_1(u,v,w) = -B_1(u,w,v)$ $\square$

Proposition 2.3.3:

If a sequence u^n in X converges weakly to an element $u \in X$, then for every $v \in X$ we have

$$\lim_{n\to\infty} B(u^n,u^n,v) = B(u,u,v).$$

Proof: We prove that every subsequence of the numerical sequence $B(u^n, u^n, v)$ has in turn a subsequence that converges to $B(u,u,v)$. We first prove the proposition for $v \in X \cap C_0^\infty(\Omega)^3$. By equation (2.7) and proposition 2.3.2 (b), the following is true

$$B(u^n,u^n,v)= B_1(u^n,u^n,v) + \epsilon \int(u_3^n u_3^n v_1 - u_1^n u_3^n v_3)dx$$

$$= - B_1(u^n,v,u^n) + \epsilon \int(u_3^n u_3^n v_1 - u_1^n u_3^n v_3)dx$$

$$= - \sum_{j=1}^{3} \int \sqrt{J} u_j^n \left(u_1^n \frac{\partial}{\partial x_1} + u_2^n \frac{\partial}{\partial x_2}\right) v_j dx + \epsilon \int(u_3^n u_3^n v_1 - u_1^n u_3^n v_3)dx$$

Since u^n is weakly convergent in X, $||u^n||$ is bounded, thus by the Sobolev compact imbedding theorem, u^n has a subsequence u^{n_k} which converges strongly in $L^2(\Omega)^3$.

Thus $u_j^{n_k} \to u_j$ in $L^2(\Omega)$ as $k \to \infty$, hence $u_j^{n_k} u_i^{n_k} \to u_j u_i$ in $L^1(\Omega)$ as

$k \to \infty$, and consequently $\sqrt{J}\, u_j^{n_k} u_i^{n_k} \frac{\partial v_j}{\partial x_i} \to \sqrt{J}\, u_j u_i \frac{\partial v_j}{\partial x_i}$ in $L^1(\Omega)$, since $v_j \in C_0^\infty(\Omega)$ and hence v_j and its derivatives are in $L^\infty(\Omega)$.

The above shows that

$$\lim_{k\to\infty} B(u^{n_k}, u^{n_k}, v) = -B_1(u,v,u) + \epsilon \int (u_3 u_3 v_1 - u_1 u_3 v_3)dx$$

$$= B_1(u,u,v) + \epsilon \int (u_3 u_3 v_1 - u_1 u_3 v_3)dx = B(u,u,v).$$

To prove the result for $v \in X$, choose $v^1 \in X \cap C_0^\infty(\Omega)^3$ such that $||v-v^1||$ is "small" and use the inequality

$$|B(u^n,u^n,v) - B(u,u,v)| \le |B(u^n,u^n,v) - B(u^n,u^n,v^1)|$$
$$+ |B(u^n,u^n,v^1) - B(u,u,v^1)| + |B(u,u,v^1) - B(u,u,v)| \qquad \square$$

Proposition 2.3.4: (apriori estimate)

A solution u of problem (Q) satisfies

(2.8) $$||u|| \le ||F||^*/\alpha$$

where α is defined by (2.3) and $||F||^* = \sup \left\{ \frac{|(F,w)^*|}{||w||} : w \in X \right\}$

Proof:

By assumption:

$$a_0(u,w) + B(u,u,w) = (F,w)^* \quad \text{for every } w \in X.$$

Choose $w = u$ and recall that $B(u,u,u) = 0$, we obtain

$$a_0(u,u) = (F,u)^*.$$

Thus $\alpha \; ||u||^2 \le ||F||^* \; ||u||$ and the result follows □

Existence now follows from the theorem below. Its proof can be found in Temam (1984) and Girault and Raviart (1979).

Theorem 2.3.5: (Existence)

Let H be a separable Hilbert space. Let a_0 be continuous, symmetric, coercive bilinear form on H, and let B be a trilinear, separately continuous form on H which satisfies

(a) $B(u,u,u) = 0$ for every $u \in H$.

(b) $\lim_{n \to \infty} B(u^n, u^n, v) = B(u,u,v)$ for $v \in H$ and a sequence u^n converging weakly to u in H.

Then for $f \in H^*$, the problem

$a_0(u,w) + B(u,u,w) = (f,w)^*$ for every $w \in H$

has a solution u in H. □

2.4: Uniqueness

Let the numbers α and β be defined by (2.3) and (2.4), and for $F \in X^*$, define

$$(2.9) \qquad ||F||^* = \sup\left\{\frac{|(F,v)^*|}{||v||} : v \in X,\ v \neq 0\right\}$$

Theorem 2.4.1: (Uniqueness)

If

$$(2.10) \qquad ||F||^* < \alpha^2/\beta$$

then the solution u of problem (Q) is unique.

Proof: Let u, v be solutions of problem (Q).

Then for every $w \in X$

$$a_0(u,w) + B(u,u,w) = (F,w)^*$$

$$a_0(v,w) + B(v,v,w) = (F,w)^*$$

subtracting the last equation from the one above we have

$$a_0(u - v,\ w) = B(v,v,w) - B(u,u,w)$$

Selecting $w = u - v$ in the above equation and using proposition 2.3.1, we obtain

$$a_0(u - v,\ u - v) = B(u - v,\ u - v,\ v)$$

By definition of α and β it follows that

$$\alpha\ ||u - v||^2 \leq \beta\ ||u - v||^2\ ||v||$$

Since v is a solution, it satisfies the apriori estimate (2.8) thus

$$\alpha \; ||u - v||^2 \leq \frac{\beta||F||^*}{\alpha} \; ||u - v||^2 \qquad \text{i.e.}$$

$$(\alpha^2 - \beta||F||^*) \; ||u - v||^2 \leq 0$$

The hypothesis of the theorem now implies that u = v. □

Remark: In our problem, the functional F is the vector $F = \begin{bmatrix} 0 \\ 0 \\ 4R \end{bmatrix}$ acting on X by integration, thus

$$(F,w)^* = \sum_{i=1}^{3} \int F_j w_j dx = 4R \int w_3 dx$$

and

$$||F||^* = 4R \sup \left\{ \frac{|\int w_3 dx|}{||w||} : w \in X, \; w \neq 0 \right\}$$

$$\leq 4R\sqrt{\pi} \sup \left\{ \frac{||w_3||_0}{||w||} : w \in X, \; w \neq 0 \right\} \leq 4R\sqrt{\pi}$$

Thus we have the following corollary which asserts the uniqueness of the solution for "small" Reynolds numbers.

Corollary: For $R < \dfrac{\alpha^2}{4\beta\sqrt{\pi}}$, the solution of problem (Q) is unique.

Chapter 3: THE APPROXIMATE PROBLEM AND ITS SOLUTION

3.1: Motivation and Statement of the Problem.

In this chapter we introduce finite element (F.E.) analogues of the continuous problems (P) and (Q). Our F.E. formulation resembles the well-known Taylor-Hood approximation of the Navier-stokes equations. References on F.E. approximation of the Navier Stokes equations include the works of Hood and Taylor (1973), Girault and Raviart (1979), Glowinski and Pironneau (1979), Bercovier and Pironneau (1979), Le Tallec (1980), and Glowinski (1984).

We use C^0 piecewise biquadratic polynomials to approximate the velocity components, and C^0 piecewise bilinear polynomials to approximate the pressure. The reference elements and their respective basis functions are shown in Figure 2.

Let the domain Ω be approximated by a union Ω_h of elementary rectangles. Observe that the unit disk Ω cannot be covered exactly by elementary rectangles, and thus $\Omega_h \neq \Omega$. In practice however, one uses isoparametric elements to accomodate the curved boundary, and since in this thesis we do not study the effect of using isoparametric elements, we shall disregard the distinction between Ω and Ω_h, and assume that $\Omega = \Omega_h$.

As is usually done in F • E • approximations, we are thinking of a family $\{\tau_h\}_h$ of tessilations of Ω, indexed by the parameter h which is the maximum diameter of an element in τ_h. We also assume that $h \to 0$. The precise assumptions on the family $\{\tau_h\}_h$ will be stated in the next chapter.

Let Q_1 and Q_2 denote respectively the spaces of bilinear and biquadratic polynomials in two variables, and define the finite element

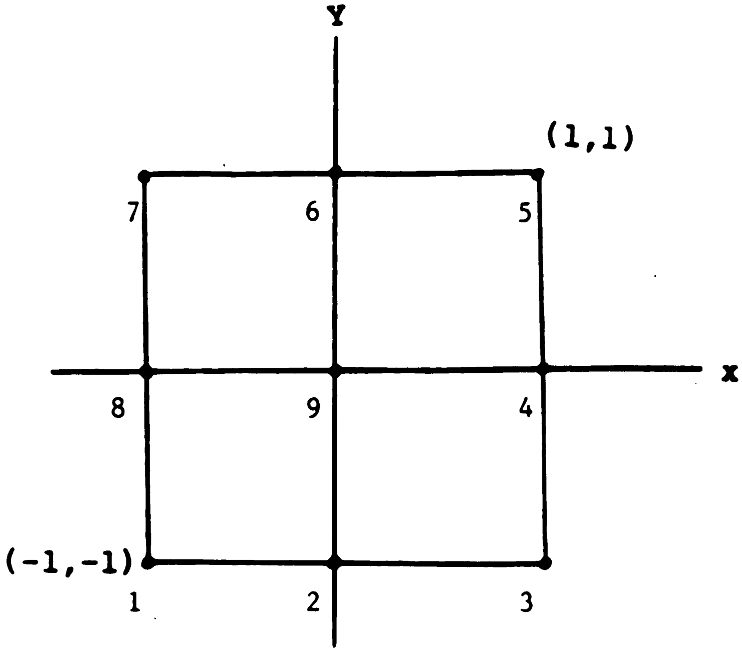

$$N_1 = x(x-1)y(y-1)/4$$
$$N_2 = -(x-1)(x+1)y(y-1)/2$$
$$N_3 = x(x+1)y(y-1)/4$$
$$N_4 = -x(x+1)(y-1)(y+1)/2$$
$$N_5 = x(x+1)y(y+1)/4$$
$$N_6 = -(x-1)(x+1)y(y+1)/2$$
$$N_7 = x(x-1)y(y+1)/4$$
$$N_8 = -x(x-1)(y-1)(y+1)/2$$
$$N_9 = (x-1)(x+1)(y-1)(y+1)$$

The reference element for the velocity and its basis functions.

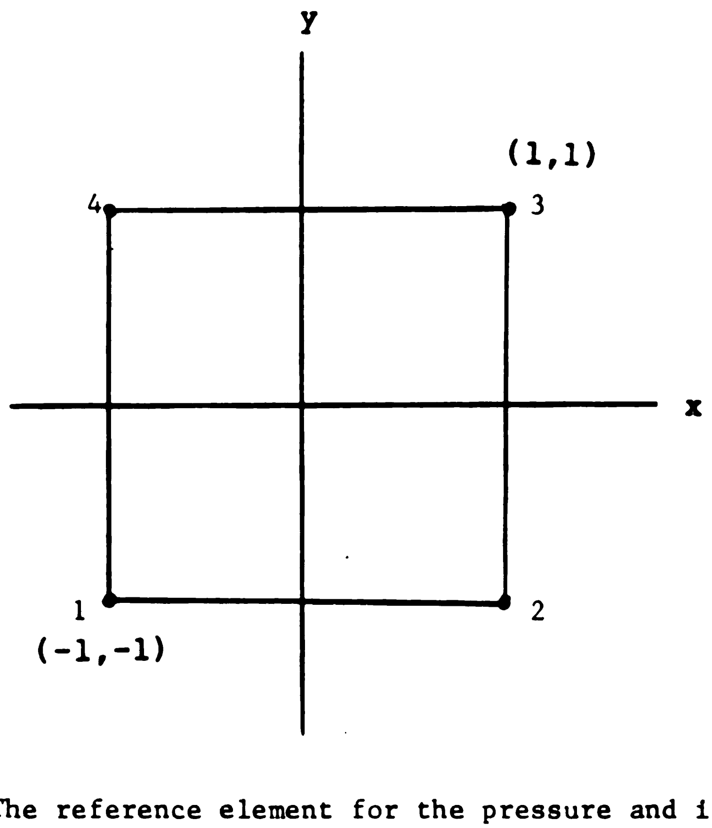

$$M_1 = (x-1)(y-1)/4$$
$$M_2 = -(x+1)(y-1)/4$$
$$M_3 = (x+1)(y+1)/4$$
$$M_4 = -(x-1)(y+1)/4$$

The reference element for the pressure and its basis functions.

The reference elements

Figure 2

spaces H^1_{0h} and M_h as follows:

(3.1) $$H^1_{0h} = \{u_h \in C^0(\overline{\Omega}): u_h\big|_e \in Q_2, \ u_h\big|_\Gamma = 0\}$$

(3.2) $$M_h = \{q_h \in C^0(\overline{\Omega}): q_h\big|_e \in Q_1, \int q_h \, dx = 0\}$$

In the above, e denotes a typical element, Γ is the boundary of Ω, and the integral in (3.2) is taken over Ω.

Observe that H^1_{0h} is a subspace of $H^1_0(\Omega)$ and that M_h is a subspace of $L^2_0(\Omega)$ (in fact is a subspace of $H^1(\Omega)$). The spaces $(H^1_{0h})^2$ and $(H^1_{0h})^3$ are defined in the obvious way. Observe that the continuity equation div $(u\sqrt{J}) = 0$ is equivalent to the condition

(3.3) $$\int q \, \text{div} \, (u\sqrt{J})dx = 0 \quad \text{for every } q \in L^2_0(\Omega)$$

and in the approximate problem we replace (3.3) by the discrete condition that the approximate velocity u_h satisfies

(3.4) $$\int q_h \, \text{div} \, (u_h\sqrt{J}) \, dx = 0 \text{ for every } q_h \in M_h$$

We now define the approximate solution space for the velocity as follows:

(3.5) $$V_{\epsilon h} = \{u_h \in (H^1_{0h})^2: \int q_h \text{div}(u_h\sqrt{J})dx = 0 \text{ for every } q_h \in M_h\}$$

(3.6) $$X_h = V_{\epsilon h} \times H^1_{0h}.$$

Remark: $V_{\epsilon h}$ is not a subspace of V_ϵ, and consequently X_h is not a subspace of X.

We now state the approximate versions of problems (P) and (Q) of chapter 2.

Problem (P_h)

Find $u_h \in (H^1_{0h})^3$ and $p_h \in M_h$ such that

$$a_0(u_h,w_h) + B(u_h,u_h,w_h) = -(\nabla p_h,\ w_h\sqrt{J})_0 + (F,w_h)^*$$

$$\text{for every } w_h \in (H^1_{0h})^3$$

$$\int q_h \operatorname{div}(u_h\sqrt{J})\,dx = 0 \qquad \text{for every } q_h \in M_h$$

Problem (Q_h)

Find $u_h \in X_h$ such that

$$a_0(u_h,w_h) + B(u_h,u_h,w_h) = (F,w_h)^*, \qquad \text{for every } w_h \in X_h.$$

As in the continuous case, we show the equivalence of (P_h), and (Q_h). To achieve this we need a discrete analogue of lemma 2.1.2 which guarantees the existence and uniqueness of the pressure.

3.2: Brezzi-type condition

The proof of the following technical lemma can be found in Bercovier and Pironneau (1979).

Lemma 3.2.1:

If every element $e \in \tau_h$ has at least one vertex which is not on the boundary of Ω, then there exists a constant $C_1 > 0$, independent of h such that

$$\sup\left\{\frac{(\nabla p_h,\ w_h)_0}{||w_h||_0}:\ w_h \in (H^1_{0h})^2,\ w_h \neq 0\right\} \geq C_1\ ||\nabla p_h||_0$$

$$\text{for all } p_h \in M_h. \qquad \square$$

Lemma 3.2.2:

If the assumption of lemma 3.2.1 holds, then for ϵ "small enough", there exists a constant C_2, independent of h such that for all $p_h \in M_h$

$$\sup\left\{\frac{(\nabla p_h,\ w_h\sqrt{J})_0}{||w_h||_0}:\ w_h \in (H^1_{0h})^2,\ w_h \neq 0\right\} \geq C_2\ ||\nabla p_h||_0 \tag{3.7}$$

Proof: Recall that $\sqrt{J} = 1 - \epsilon x_1$, $|x_1| \leq 1$, thus

$$\frac{(\nabla p_h,\ w_h\sqrt{J})_0}{||w_h||_0} = \frac{(\nabla p_h,\ w_h)_0}{||w_h||_0} - \epsilon\,\frac{(\nabla p_h,\ x_1 w_h)_0}{||w_h||_0} \geq$$

$$\frac{(\nabla p_h,\ w_h)_0}{||w_h||_0} - \epsilon\,\frac{|(\nabla p_h,\ x_1 w_h)_0|}{||w_h||_0} \geq \frac{(\nabla p_h,\ w_h)_0}{||w_h||_0} - \epsilon\,\frac{||\nabla p_h||_0\ ||x_1 w_h||_0}{||w_h||_0} \geq$$

$$\frac{(\nabla p_h,\ w_h)_0}{||w_h||_0} - \epsilon\ ||\nabla p_h||_0$$

Thus by lemma 3.2.1 we have,

$$\sup \left\{ \frac{(\nabla p_h,\ w_h\sqrt{J})_0}{||w_h||_0} :\ w_h \in (H^1_{0h})^2,\ w_h \neq 0 \right\} \geq$$

$$\sup \left\{ \frac{(\nabla p_h,\ w_h)_0}{||w_h||_0} :\ w_h \in (H^1_{0h})^2,\ w_h \neq 0 \right\} - \epsilon\ ||\nabla p_h||_0 \geq$$

$$(C_1 - \epsilon)\ ||\nabla p_h||_0$$

Now take $\epsilon < C_1$, and set $C_2 = C_1 - \epsilon$. □

3.3: The Equivalence of (P_h) and (Q_h)

Lemma 3.2.2 now implies the equivalence of (P_h) and (Q_h):

Define $L_{\epsilon h}: (H^1_{0h})^3 \to M^*_h$ by $(L_{\epsilon h} w_h, p_h)^* = \int p_h \operatorname{div} (w_h\sqrt{J})dx$.
Then the adjoint $L^*_{\epsilon h}: M_h \to ((H^1_{0h})^3)^*$ is defined by

$$(L^*_{\epsilon h} p_h, w_h)^* = -\ (\nabla p_h,\ w_h\sqrt{J})_0$$

Condition 3.7 implies that $L^*_{\epsilon h}$ is one-to-one, and hence $L_{\epsilon h}$ maps $(H^1_{0h})^3$ onto M^*_h. Now the proof of the following equivalence theorem is exactly like that of proposition 2.2.3.

Theorem 3.3.1:

Problems (P_h) and (Q_h) are equivalent in the following sense: If $(u_h,\ p_h) \in X_h \times M_h$ is a solution of (P_h), then u_h is also a solution of

(Q_h). Conversely if u_h is a solution of (Q_h), then there exists a unique $p_h \in M_h$ such that the pair (u_h, p_h) is a solution of (P_h). □

Remarks:

(a) The space X_h is the kernel of the linear operator $L_{\epsilon h}$, and thus if N is the number of interior mesh points for the velocities, and $M(< N)$ is the number of mesh points for the pressure, then M_h has dimension $M-1$, $(H^1_{0h})^3$ has dimension $3N$ and X_h has dimension $3N - M + 1$.

(b) Let $\{N_j\}_{j=1}^{N}$, $\{M_i\}_{i=1}^{M-1}$ be the basis functions for H^1_{0h} and M_h respectively. Define a matrix $D = (D^1, D^2)$ by

(3.8) $$D^1_{ij} = \int N_j \frac{\partial M_i}{\partial x_1} \sqrt{J}\, dx$$

(3.9) $$D^2_{ij} = \int N_j \frac{\partial M_i}{\partial x_2} \sqrt{J}\, dx$$

$$1 \le i \le M-1, \quad 1 \le j \le N$$

Then condition (3.7) implies that the matrix D has full rank $(M - 1)$

3.4: The Solution of the Approximate Problem.

We turn now to the question of existence and uniqueness of the approximate problem (Q_h). Observe that the restriction of the trilinear form B to the space X_h does not have the properties given in proposition 2.3.1, because the space X_h is not a subspace of X, and thus the elements of X_h do not satisfy the continuity equation exactly.

This makes problem (Q_h) more difficult to study since for example the apriori estimate (2.8) is no longer valid for the solution of (Q_h). However, at the additional cost of restricting the size of the forcing term $||F||^*$ more than we need for uniqueness (Condition (2.10) in theorem 2.4.1), we can show that problem (Q_h) has a unique solution u_h which satisfies the same apriori estimate as the exact solution u.

The following condition is a standing assumption in this chapter and the following one:

$$(3.10) \qquad ||F||^* < \frac{\alpha^2}{4\beta}$$

where α and β are defined by equation (2.3) and (2.4).

Definition: For $||F||^* < \frac{\alpha^2}{4\beta}$, let

$$(3.11) \qquad r = (\alpha - \sqrt{\alpha^2 - 4\beta||F||^*}) \;/\; 2\beta$$

Observe that r is the smaller zero of the quadratic equation $\beta r^2 - \alpha r + ||F||^* = 0$, and that

$$(3.12) \qquad \alpha - \beta r > 0$$

$$(3.13) \qquad \alpha - 2\beta r > 0$$

$$(3.14) \qquad k = \frac{\beta||F||^*}{(\alpha-\beta r)^2} < 1$$

Observe also that when condition (3.10) is satisfied, the exact solution u of the continous problem in unique, and by (2.8) it follows that

$$(3.15) \qquad ||u|| \leq \frac{||F||^*}{\alpha} = r - \frac{\beta r^2}{\alpha} < r$$

Thus the exact solution lies in the ball

$$D_r = \{u \in H_0^1(\Omega)^3 : \ ||u|| \leq r\}$$

This suggests that we look for an approximate solution in D_r, and indeed there is a unique solution of (Q_h) in D_r.

We begin with the following

Lemma 3.4.1:

For $u_h \in X_h$, $||u_h|| \leq r$, and for any $\ell \in X_h^*$, the problem

$$a_o(v_h,w_h) + B(u_h,v_h,w_h) = (\ell,w_h)^* \quad \text{for every } w_h \in X_h$$

has a unique solution v_h.

Proof: The result follows from the Lax- Milgram theorem, since for all $v_h \in X_h$ we have

$$a_o(v_h,v_h) + B(u_h,v_h,v_h) \geq (\alpha-\beta||u_h||)||v_h||^2 \geq (\alpha-\beta r) \ ||v_h||^2$$

and $\alpha - \beta r > 0$ by (3.12). □

The above lemma allows us to make the following definition. Define a mapping Φ: $D_r \to X_h$ by $\Phi(u_h) = v_h$, where v_h is the unique solution of

(3.16) $\quad a_o(v_h, w_h) + B(u_h, v_h, w_h) = (F, w_h)^* \text{ for every } w_h \in X_h$

Lemma 3.4.2:

The mapping Φ defined above maps D_r into D_r.

Proof: If we choose $w_h = v_h$ in (3.16) we obtain

$$||v_h||^2(\alpha - \beta r) \le a_o(v_h, v_h) + B(u_h, v_h, v_h) = (F, v_h)^* \le ||F||^* \, ||v_h||.$$

Thus $||v_h|| \le \dfrac{||F||^*}{\alpha - \beta r} = r$ $\quad\square$

Remark: Observe that every solution of problem (Q_h) is a fixed point of Φ.

Proposition 3.4.3:

Φ is a contraction on D_r.

Proof: For $u_h \in D_r$, define $Au_h \in \mathcal{L}(X_h, X_h^*)$ by

$$(Au_h(v_h), w_h)^* = a_0(v_h, w_h) + B(u_h, v_h, w_h).$$

$$||Au_h(v_h)||^* = \sup\left\{\frac{|a_0(v_h, w_h) + B(u_h, v_h, w_h)|}{||w_h||}: w_h \in X_h,\ w_h \neq 0\right\} \ge$$

$$\frac{|a_0(v_h, v_h) + B(u_h, v_h, v_h)|}{||v_h||} \ge \frac{a(v_h, v_h) - |B(u_h, v_h, v_h)|}{||v_h||} \ge$$

$$(\alpha - \beta||u_h||)\ ||v_h|| \geq (\alpha - \beta r)\ ||v_h||$$

Since $\alpha - \beta r > 0$ (by 3.12), Au_h is bounded away from zero, and is therefore one-to-one.

Lemma 3.4.1 states that Au_h is also onto. The open mapping theorem implies that Au_h has a bounded inverse Au_h^{-1} and that

$$(3.17) \qquad ||Au_h^{-1}|| \leq \frac{1}{\alpha - \beta r}$$

Observe that now by definition $\Phi(u_h) = Au_h^{-1}F$. We now show that Φ is a contraction: let u_h^1, u_h^2 be in D_r, and let

$$A_i = Au_h^i \qquad (i = 1,2).$$

We have $A_2^{-1} - A_1^{-1} = A_2^{-1}(A_1 - A_2)A_1^{-1}$, thus by (3.17)

$$(3.18) \qquad ||A_2^{-1} - A_1^{-1}|| \leq \frac{1}{(\alpha-\beta r)^2}\ ||A_1 - A_2||$$

It is easy to check that $||A_1 - A_2|| \leq \beta\ ||u_h^1 - u_h^2||$.
Now $||\Phi(u_h^2) - \Phi(u_h^1)|| = ||A_2^{-1}F - A_1^{-1}F|| \leq ||A_2^{-1} - A_1^{-1}||\ ||F||^* \leq$
$\dfrac{\beta||F||^*}{(\alpha-\beta r)^2}\ ||u_h^2 - u_h^1|| = k||u_h^2 - u_h^1||$,

where $k < 1$ is defined by (3.14) □

Theorem 3.4.4: Problem (Q_h) has a unique solution u_h in D_r.

Proof: The result follows directly from proposition 3.4.3 and the remark preceeding it. □

3.5: A Fixed Point Scheme.

Proposition 3.4.3 provides the following practical scheme for finding the solution u_h of (Q_h). Choose an initial approximation $u_h^0 \in X_h \cap D_r$, and define a sequence $\{u_h^n\}$ $(n \geq 1)$, converging to u_h by $u_h^{n+1} = \Phi(u_h^n)$ i.e. given u_h^n, u_h^{n+1} is the solution of the linear problem $u_h^{n+1} \in X_h$,

$$(3.18)\quad a_0(u_h^{n+1}, w_h) + B(u_h^n, u_h^{n+1}, w_h) = (F, w_h)^* \text{ for every } w_h \in X_h.$$

Again by an argument similar to the proof of proposition 2.2.3 it is easy to show that lemma 3.2.2 can be used to show that problem (3.18) is equivalent to the following problem.

Given $u_h^n \in X_h \cap D_r$, find $u_h^{n+1} \in (H_{0h}^1)^3$, $p_h^{n+1} \in M_h$ such that

$$(3.19)\quad a_o(u_h^{n+1}, w_h) + B(u_h^n, u_h^{n+1}, w_h) = -(\nabla p_h^{n+1}, w_h\sqrt{J})_0 + (F, w_h)^*$$

$$\text{for every } w_h \in (H_{0h}^1)^3$$

$$(3.20)\qquad \int q_h \operatorname{div}(u_h^{n+1}\sqrt{J})dx = 0 \quad \text{for every } q_h \in M_h$$

Observe that the solution of (3.19), (3.20) can be obtained by solving a linear system of algebraic equations which is constructed as follows:

let $\{N_i\}_{i=1}^{N}$ be the basis functions for H_{0h}^1 and let $\{M_j\}_{j=1}^{M-1}$ be the basis functions for M_h, then the space $(H_{0h}^1)^3$ has the basis

$$(3.21) \qquad \{(N_i,0,0),\ (0,N_i,0),\ (0,0,N_i)\}_{i=1}^{N}$$

Clearly, equations (3.19) is satisfied for all $w_h \in (H^1_{0h})^3$ if and only if it is satisfied for all the basis functions (3.21). The same applies to equation (3.20) and the basis functions M_j. Thus if we substitute the basis functions (3.21) in (3.19), we obtain 3 sets of linear systems each containing N equations. Simiarly (3.20) gives rise to a system of M-1 equations. The combined system of 3N + M - 1 equations can then be solved for the nodal values of the velocities and the pressure. The matrix of the system described above will be referred to as the grand fluid matrix. As an illustration, let us describe explicity the equations that correspond to using $w_h = (0,0,N_i)$ in equations (3.19).

Let $u_h^{n+1} = (u_{1h}^{n+1}\ ,\ u_{2h}^{n+1},\ u_{3h}^{n+1})$, where for example

$$u_{3h}^{n+1} = \sum_{j=1}^{N} u_{3j}N_j, \text{ and let } U_3^{n+1} = (u_{31}, \ . \ . \ . \ ., u_{3N})^T$$

be the nodal values of u_{3h}^{n+1}. The substitution $w_h = (0,0,N_i)$, $1 \leq i \leq N$, yields the matrix equation

$$(3.22) \qquad A_3^{n+1}\ U_3^{n+1} = G$$

where G is the column vector whose i^{th} component is $(F,(0,0,N_i))^*$, and the (i,j) entry of A_3^{n+1} is

$$\int \sqrt{J}\ \nabla N_i \cdot \nabla N_j + \left(\frac{\epsilon^2}{\sqrt{J}} - \epsilon u_1^n\right)N_iN_j + \sqrt{J}\ N_i\left(u_1^n \frac{\partial N_j}{\partial x_1} + u_2^n \frac{\partial N_j}{\partial x_2}\right)\, dx.$$

Similar equations can be derived by substituting $(N_i, 0, 0)$, $(0, N_i, 0)$ in (3.19) and M_j in (3.20). Observe that equation (3.22) involves the nodal values of u_{3h}^{n+1} only, and thus the grand fluid matrix can be rearranged into a block diagonal matrix. Observe also that this is no coincidence, indeed the triliniear form B was defined in such a way to guarantee this nice feature of the grand fluid matrix. Other definitions of B are possible, and for some of these definitions, the existence proof given in chapter 2 can be greatly simplified, however, such definitions lead to more dense matrices than the one described above. The reader is referred to Taylor and Hughes (1981) for more details on the computer implementation of F.E. method in flow problems.

3.6: The discrete Stokes Problem.

The continuous stokes problem associated with the flow under investigation has the form

(SP) Find $u \in H_0^1(\Omega)^3$ and $p \in L_0^2(\Omega)$ such that

$$a_0(u, w) = -(\nabla p, w\sqrt{J})^* + (F, w)^* \text{ for every } w \in H_0^1(\Omega)^3,$$

$$\operatorname{div}(u\sqrt{J}) = 0$$

Again problem (SP) can be shown to be equivalent to the problem

(SQ) Find $u \in X$ such that

$$a_0(u, w) = (F, w)^* \quad \text{for every } w \in X.$$

Problem (SQ) has a unique solution by the Lax-Milgram theorem. The discrete form of problems (SP) and (SQ) will have great importance in chapters 4 and 5, and hence deserve the brief description we give below.

If we use the same F.E. approximations of u, p as was done in section 3.1, one obtains the discrete versions of problems (SP) and (SQ):

(SP_h) Find $u_h \in (H^1_{0h})^3$ and $p_h \in M_h$ such that

$$a_o(u_h, w_h) = -(\nabla p_h, w_h\sqrt{J})_0 + (F, w_h)^* \quad \text{for every } w_h \in (H^1_{0h})^3.$$

$$\int q_h \operatorname{div}(w_h\sqrt{J})dx = 0 \quad \text{for every } q_h \in M_h.$$

(SQ_h) Find $u_h \in X_h$ such that

$$a_0(u_h, w_h) = (F, w_h)^* \qquad \text{for every } w_h \in X_h$$

Equations (SP_h) lead to the following system of linear equations for the nodal values U_1, U_2, U_3 and P of u_{1h}, u_{2h}, u_{3h} and p_h respectively.

$$(3.23) \qquad \begin{bmatrix} A & 0 & (D^1)^T & 0 \\ 0 & A^1 & (D^2)^T & 0 \\ D^1 & D^2 & 0 & 0 \\ 0 & 0 & 0 & A \end{bmatrix} \begin{bmatrix} U_1 \\ U_2 \\ P \\ U_3 \end{bmatrix} = \begin{bmatrix} G_1 \\ G_2 \\ 0 \\ G_3 \end{bmatrix}$$

where the ith components of G_1, G_2, G_3 are given by

$$(G_1)_i = (F, (N_i, 0, 0))^*,$$

$$(G_2)_i = (F, (0, N_i, 0))^*$$

$(G_3)_i = (F, (0,0,N_i)^*$

D^1 and D^2 are defined by (3.8) and (3.9), and the (i,j) extries of A and A^1 are

$$A_{ij} = \int(\nabla N_i \cdot \nabla N_j \sqrt{J} + \frac{\epsilon^2}{\sqrt{J}} N_i N_j)dx,$$

$$A^1_{ij} = \int \nabla N_i \cdot \nabla N_j \sqrt{J}\, dx.$$

Observe that $D = (D_1, D_2)$ has full rank, and that A and A^1 are symmetric, positive definite, and by numbering the mesh nodes appropriately A and A^1 are banded with the band width considerably smaller then the size of these matrices. The practicalities involved in solving (3.23) are outlined in appendix B.

CHAPTER 4: ERROR ANALYSIS

In this chapter we give an error bound on $||u-u_h||$, where throughout the chapter, u will denote the exact solution, and u_h will denote the solution of the approximate problems (P_h) and (Q_h).
Thus $u \in X$ satisfies the equations

(4.1) $$a_o(u,w) + B(u,u,w) = (p, \mathrm{div}(w\sqrt{J}))_0 + (F,w)^*$$

$$\text{for every } w \in H_0^1(\Omega)^3.$$

(4.2) $$a_o(u,w) + B(u,u,w) = (F,w)^* \text{ for every } w \in X,$$

and $u_h \in X_h$ satisfies the equations

(4.3) $$a_o(u_h,w_h) + B(u_h,u_h,w_h) = -(\nabla p_h, w_h\sqrt{J})_0 + (F,w_h)^*$$

$$\text{for every } w_h \in (H_{0h}^1)^3$$

(4.4) $$a_o(u_h,w_h) + B(u_h,u_h,w_h) = (F,w_h)^* \text{ for every } w_h \in X_h.$$

It will be assumed that $||F||^* < \frac{\alpha^2}{4\beta}$, thus u is the unique element of X that satisfies (4.1) and (4.2), and u_h is the unique solution of (4.3) and (4.4) that satisfies

(4.5) $$||u_h|| \leq r.$$

Observe that under the assumption that $||F||^* < \frac{\alpha^2}{4\beta}$, the exact solution u also satisfies

(4.6) $$||u|| \leq r.$$

We also assume that the hypotheses of lemma 3.2.2 are satisfied, thus ϵ is small enough to allow condition (3.7) to hold. We quote condition (3.7) here for the ease of reference:

There exists a constant $C_2 > 0$, independent of h such that

(4.7) $$\sup \left\{ \frac{(\nabla p_h \cdot w_h\sqrt{J})_0}{||w_h||_0} : w_h \in (H^1_{0h})^3,\ w_h \neq 0 \right\} \geq C_2\ ||\nabla p_h||_0$$

for all $p_h \in M_h$.

In the sequel we will continue using the letter C to denote (possibly) different positive constants, however when a specific condition such as (4.7) is used, the constant C_2 will be used to call the reader's attention to the specific condition used. We assume that our family $\{\tau_h\}_h$ of tessilations of Ω is regular in the sense of Ciarlet (1978), thus if h_e denotes the diameter of element $e \in \tau_h$, and ρ_e denoted the diameter of the largest circle that can be inscribed in e, then

(i) There exists a constant $\sigma > 0$ such that for every $e \in \tau_h$ and every τ_h

$$\frac{h_e}{\rho_e} \leq \sigma$$

(ii) The quantity $h = \max \{ h_e : e \in \tau_h\}$ approaches zero.

Besides the regularity of the $\{\tau_h\}_h$, we also assume that $\{\tau_h\}_h$ satisfies the inverse assumption:

(iii) There exists a constant $\nu > 0$ such that for every $e \in \tau_h$ and every τ_h

$$\frac{h}{h_e} \leq \nu$$

Observe that conditions (i) - (iii) are by no means restrictive in practice. We begin by stating the following lemma whose proof can be found in Ciarlet (1978)

Lemma 4.1.

Under assumptions (i) - (iii), there exists a constant $C_3 > 0$, independent of h such that

$$(4.8) \qquad \inf \left\{ \frac{||w_h||_0}{||w_h||_1} : w_h \in (H^1_{0h})^2,\ w_h \neq 0 \right\} \geq C_3 h \qquad \square$$

Lemma 4.2

For $u \in X$, there exists a constant $C > 0$, independent of h such that

$$(4.9) \qquad \inf \{||u-v_h||: v_h \in X_h\} \leq$$

$$C \inf \{||u-v_h|| + \frac{1}{h}||u-v_h||_0 : v_h \in (H^1_{0h})^3\}$$

Proof: Fix $v_h \in (H^1_{0h})^3$, and let $(z_h, \pi_h) \in X_h \times M_h$ be the solution of the discrete stokes problem

$$(4.10)\quad a_o(z_h, w_h) = -(\nabla \pi_h, w_h\sqrt{J})_0 + a_0(v_h, w_h) \text{ for every } w_h \in (H^1_{0h})^3$$

$$(4.11)\quad (\nabla q_h, z_h\sqrt{J})_0 = 0 \text{ for every } q_h \in M_h$$

The boundedness of a_0 yields

$$(4.12)\quad ||v_h - z_h|| \geq C \sup\left\{\frac{a_0(v_h - z_h, w)}{||w||} : w \in H^1_0(\Omega)^3,\ w \neq 0\right\} \geq$$

$$C \sup\left\{\frac{a_0(v_h - z_h, w_h)}{||w_h||} : w_h \in (H^1_{0h})^3,\ w_h \neq 0\right\} =$$

$$C \sup\left\{\frac{(\nabla \pi_h, w_h\sqrt{J})_0}{||w_h||} : w_h \in (H^1_{0h})^3,\ w_h \neq 0\right\}$$

where the last equality in (4.12) is by (4.10). (4.12) yields

$$(4.13)\quad ||v_h - z_h|| \geq C \sup\left\{\frac{(\nabla \pi_h, w_h\sqrt{J})_0}{||w_h||} : w_h \in (H^1_{0h})^2,\ w_h \neq 0\right\} \geq$$

$$C \sup\left\{\frac{(\nabla \pi_h, w_h\sqrt{J})_0}{||w_h||_0} : w_h \in (H^1_{0h})^2\right\} \inf\left\{\frac{||w_h||_0}{||w_h||} : w_h \in (H^1_{0h})^2\right\}$$

Now (4.13), (4.7) and (4.8) give

$$(4.14)\quad ||v_h - z_h|| \geq C\, C_2 C_3\, ||\nabla \pi_h||_0 \cdot h$$

We rename $C\ C_2\ C_3$ to C. Using (4.14), the ellipticity of a_0, and (4.10) respectively we have

$$(4.15)\quad h||v_h-z_h|| \le C\,\frac{||v_h - z_h||^2}{||\nabla\pi_h||_0} \le C\,\frac{a_0(v_h-z_h,\ v_h-z_h)}{||\nabla\pi_h||_0} =$$

$$C\,\frac{(\nabla\pi_h,\ (v_h-z_h)\sqrt{J})_0}{||\nabla\pi_h||_0}$$

(4.15), (4.11), and the fact that $u \in X$ imply

$$h||v_h-z_h|| \le C\,\frac{(\nabla\pi_h,\ (v_h-u)\sqrt{J})_0}{||\nabla\pi_h||_0}$$

Thus

$$(4.16)\quad h||v_h-z_h|| \le C\sup\left\{\frac{(\nabla\pi_h,\ (v_h-u)\sqrt{J})_0}{||\nabla\pi_h||_0} :\ \pi_h \in M_h\right\} \le$$

$$C\sup\left\{\frac{(w,(v_h-u)\sqrt{J})_0}{||w||_0} :\ w \in L^2(\Omega)^2\right\} = C\ ||(v_h-u)\sqrt{J}||_0 \le C\ ||v_h-u||_0$$

where the last inequality in (4.16) is by the boundedness of $\sqrt{J}$. By the triangle inequality and (4.16) we have

$$||u-z_h|| \le ||u-v_h|| + ||v_h-z_h|| \le ||u-v_h|| + \frac{C}{h}\,||u-v_h||_0$$

and this implies (4.9) and completes the proof. □

Theorem 4.3:

Under the assumptions stated before lemma (4.1), there exists a constant $C > 0$ such that

$$||u-u_h|| \le Ch^2$$

Proof:

$$\text{Fix } v_h \in X_h, \text{ and let } w_h = u_h - v_h.$$

Consider the expression

$$E = a_0(w_h, w_h) + B(w_h, u_h, w_h)$$

By (2.3), (2.4) and (4.5) we have

$$E \ge (\alpha - \beta r)||w_h||^2 \tag{4.17}$$

By (4.4) and the definition of E we have

$$\begin{aligned} E &= a_0(u_h, w_h) - a_0(v_h, w_h) + B(w_h, u_h, w_h) = \\ &-B(u_h, u_h, w_h) + (F, w_h)^* - a_0(v_h, w_h) + B(w_h, u_h, w_h) = \\ &(F, w_h)^* - B(v_h, u_h, w_h) - a_0(v_h, w_h) \end{aligned} \tag{4.18}$$

(4.18) and (4.1) yield

$$\begin{aligned} E = &-(p, \mathrm{div}(w_h\sqrt{J}))_0 + a_0(u, w_h) + B(u, u, w_h) \\ &- a_0(v_h, w_h) - B(v_h, u_h, w_h) \end{aligned} \tag{4.19}$$

Using the fact that $w_h \in X_h$, a simple manipulation of (4.19) gives

$$(4.20)\quad E = -(p-q_h, \mathrm{div}(w_h\sqrt{J}))_0 + a_0(u-v_h, w_h) + B(u-v_h, u_h, w_h)$$
$$+ B(u, u-u_h, w_h)$$

where $q_h \in M_h$ is arbitrary. It now follows from (4.20), (4.5), (4.6) and the triangle inequality that

$$(4.21)\quad E \le C||w_h||\ ||p-q_h||_0 + C||w_h||\ ||u-v_h|| + \beta r||w_h||\ [||u-v_h|| +$$
$$||u-u_h||] \le C\ ||w_h||\ ||p-q_h||_0 + C||w_h||\ ||u-v_h|| + 2\beta r\ ||w_h||\ ||u-v_h||$$
$$+ \beta r||w_h||^2$$

Now (4.17) and (4.21) yield

$$(\alpha-2\beta r)\ ||w_h||^2 \le C\ ||w_h||\ [||p-q_h||_0 + ||u-v_h||] \text{ i.e.}$$

$$(4.22)\qquad ||w_h|| \le \frac{C}{(\alpha-2\beta r)}[||p-q_h||_0 + ||u-v_h||]$$

Observe that $\alpha - 2\beta r > 0$ by (3.13). Now the triange inequality and (4.22) give

$$||u-u_h|| \le ||u-v_h|| + ||v_h-u_h|| \le C[||p-q_h||_0 + ||u-v_h||]$$

for every $v_h \in X_h$, and every $q_h \in M_h$.

Thus

$$(4.23)\quad ||u-u_h|| \le C \inf \{||p-q_h||: q_h \in M_h\} + C \inf \{||u-v_h||: v_h \in X_h\}$$

(4.23) and (4.9) give

$$(4.24)\qquad ||u-u_h|| \le C \inf \{||p-q_h||_0: q_h \in M_h\}$$

$$+ C \inf \{||u-v_h|| + \frac{1}{h}||u-v_h||_0: v_h \in (H^1_{0h})^3\}$$

Now the result follows from (4.24) if we choose for v_h the interpolant $\Pi_h u$ of u in $(H^1_{0h})^3$ and for q_h the interpolant $\Pi_h p$ in M_h. By the general interpolation theory in Sobolev spaces (see e.g. Ciarlet (1978), Oden and Carey (1983)) we have

$||u-\Pi_h u|| = O(h^2)$, $||u - \Pi_h u||_0 = O(h^3)$, $||p-\Pi_h p||_0 = O(h^2)$, and the proof is complete. □

Remark: The results quoted above require that $u \in H^3(\Omega)$, $p \in H^2(\Omega)$. Although our results in chapter 2 do not include a study of the regularity of solution (u,p), we believe that the solution is actually in $C^\infty(\Omega)$. This is intuitively obvious since the domain Ω is bounded, $\partial\Omega \in C^\infty$, and the data (boundary and forcing) are all C^∞.

5.1: Introduction

In section 3.5 we described an iterative scheme to solve the nonlinear problems (P_h) and (Q_h). Each step of the iteration required the solution of a large system of linear equations, but unfortunately the coefficient matrix used to solve for u_h^{n+1} was dependent on the previous approximation u_h^n. Thus at each step of the fixed point scheme (3.19) one must form and solve a different set of linear equations. This turned out to be rather expensive since we were interested in computing the solution over a wide range of values of R and ϵ.

In this chapter, we give an alternative scheme for solving the nonlinear equations (P_h) and (Q_h). The method described here is a straightforward extension of the techniques described in Glowinski (1984). Our discussion will be brief since this method of solution is well described in the above cited reference.

5.2: A least squares formulation

The assumptions and notations of chapter 3 will be maintained here. Probelm (Q_h) can be converted into a minimization problem as follows:

For a fixed $u_h \in X_h$, define an element $\xi_h \in X_h$ to be the solution of the discrete Stokes problem

$\xi_h \in X_h$ is such that for every $\eta_h \in X_h$ we have

$$(5.1) \qquad a_0(\xi_h,\eta_h) = a_0(u_h,\eta_h) + B(u_h,u_h,\eta_h) - (F,\eta_h)^*$$

Problem (5.1) will be referred to as the state equation, and ξ_h will be termed the state variable that corresponds to u_h. Observe that the right hand side of (5.1) is a linear functional in η_h, and thus (5.1) is a perfectly well-defined (discrete) Stokes problem whose solution ξ_h exists and is unique by the ellipicity of a_0. We now define a functional $J_h: X_h \to X_h$ by

$$J_h(u_h) = \frac{1}{2} a_0(\xi_h, \xi_h) \tag{5.2}$$

where $\xi_h = \xi_h(u_h)$ is the solution of the state equation (5.1). The proof of the following proposition is obvious if one assumes that problems (P_h) and (Q_h) have solutions which is the case for example if $||F||^* < \alpha^2/4\beta$.

Proposition 5.2.1:

An element $u_h \in X_h$ is a (global) minimizer of J_h if and only if u_h is a solution of problems (P_h) and (Q_h). □

As a corollary of the above proposition, J_h has a unique global minimizer $u_h \in D_r$ which is also the unique solution of (P_h) and (Q_h) in D_r (here we again assume that $||F||^* < \frac{\alpha^2}{4\beta}$). Now instead of solving (Q_h), we try to solve the following minimization problem:

(M_h) Find $u_h \in X_h$ such that

$$J_h(u_h) \leq J_h(v_h) \quad \text{for every } v_h \in X_h.$$

5.3: A conjugate gradient scheme.

Following Glowinski (1984), we use the following conjugate gradient scheme to solve the minimization problem (M_h). Let $u_h^0 \in X_h$ be an initial approximation of u_h, and let $z_h^0 \in X_h$ be the solution of the "linear variational equation"

$$(5.3) \qquad a_o(z_h^0, \eta_h) = \langle J_h'(u_h^0), \eta_h \rangle \quad \text{for every } \eta_h \in X_h.$$

Set $w_h^0 = z_h^0$. For $m \geq 0$, compute u_h^{m+1}, z_h^{m+1}, w_h^{m+1} as follows

Step 1 (Descent)

Compute

$$(5.4) \qquad \lambda_m = \operatorname{Argmin} \{J_h(u_h^m - \lambda w_h^m),\ \lambda \in \mathbb{R}\}$$

and set

$$(5.5) \qquad u_h^{m+1} = u_h^m - \lambda_m w_h^m$$

Step 2 (New descent direction)

Define z_h^{m+1} to be the solution of the linear variational equation

$$(5.6) \qquad a_o(z_h^{m+1}, \eta_h) = \langle J_h'(u_h^{m+1}), \eta_h \rangle \quad \text{for every } \eta_h \in X_h$$

$$(5.7) \qquad \text{Set } \gamma_{m+1} = \frac{a_0(z_h^{m+1}, z_h^{m+1} - z_h^m)}{a_0(z_h^m, z_h^m)}$$

$$(5.8) \qquad \text{and } w_h^{m+1} = z_h^{m+1} + \gamma_{m+1} w_h^m$$

Replace m by m+1 and go to (5.4). □

In equations (5.3) and (5.6), $J_h'(v_h)$ denotes the Frechet derivative of J_h at $v_h \in X_h$ defined by $\langle J_h'(v_h), \eta_h \rangle = \lim_{t \to 0} \dfrac{J_h(v_h + t\eta_h) - J_h(v_h)}{t}$

$(\eta_h \in X_h)$. It can be easily shown that

$$(5.9) \qquad \langle J_h'(v_h), \eta_h \rangle = a_0(\xi_h, \eta_h) + B(\eta_h, v_h, \xi_h) + B(v_h, \eta_h, \xi_h)$$

where $\xi_h = \xi_h(v_h)$ is the state variable corresponding to v_h.

Observe that the linear variational equation (5.6) is a discrete Stokes problem for the unknown function z_h^{m+1}. Observe that computing z_h^{m+1} actually requires the solutions of two Stokes problems: first of all, one must compute the state variable $\xi_h(u_h)$ in order to use (5.9) to compute the right hand side of (5.6), and then solve the Stokes problem (5.6) for z_h^{m+1} once $\langle J_h'(u_h^m), \eta_n \rangle$ is known. The one dimensional minimization problem (5.4) deserves a brief comment since it is in fact the most expensive step in the above scheme. Given u_h^m, w_h^m, define a real valued function

$$g(\lambda) = J_h(u_h^m - \lambda w_h^m) \qquad \lambda \in \mathbb{R}$$

and to find the minimizer λ_m in (5.4), we solve equation

$$(5.10) \qquad g'(\lambda) = 0$$

Observe that

$$(5.11) \qquad g'(\lambda) = - \langle J'(u_h^m - \lambda w_h^m), w_h \rangle$$

In our implementation of the above scheme, we used the modified false position method to solve equation (5.10). Observe that each evaluation of $g'(\lambda)$ (through (5.11)) requires the solution of one Stokes problem to find the state variable ξ_h corresponding to $u_h^m - \lambda w_h^m$, which is needed in evaluating the right hand side of (5.9). Consequently the solutions of several Stokes problems must be computed in order to find λ_m.

It must be noted that although the conjugate gradient scheme requires the solution of many Stokes problems in each iteration, it is actually a very efficient scheme since only the forcing term needs to be computed each time, but the bilinear form $a_o(. , .)$ is the same for all the the Stokes problems needed to implement the above scheme. This amounts to computing the matrix in equations (3.23) only once throughout the entire computation, and once this has been done, solving the Stokes problem only requires a back substitution to find the nodal values of the velocity and pressure.

Solving the matrix equation (3.23) associated with ths discrete Stokes problem is outlined in Appendix B.

CHAPTER 6: NUMERICAL RESULTS

6.1 Computational procedure

As we mentioned in section 1.4, the main objective of this work is to find accurate approximations of equations (1.5) - (1.8). To achieve this goal, we implemented the schemes described in chapters 3 and 5 to compute the solution u_h of problems (P_h) and (M_h) respectively. Since an initial approximation is needed in both cases, the approximate solution u_h was computed for a sequence of values of R (keeping ϵ fixed), starting at the initial value R = 25 and increments ΔR = 25. The initial approximation for R = 25 was chosen to be zero, and after the solution for a certain value of R has converged, R was incremented and the solution for the previous value of R was used as an initial approximation for the next value of R. This procedure was repeated until the final desired value of R was reached.

The above procedure was carried out for ϵ = .1, .2, ..., .5 and for values of R ranging from R = 25 to R = 1118.03.

The criterion

$$\text{(6.1)} \qquad \max \left\{ \frac{|u_{jh}^{n+1}(i) - u_{jh}^{n}(i)|}{|u_{jh}^{n}(i)|} \right\} < 10^{-3}$$

was used as an indication that the sequence u_h^n has converged to the solution u_h.

In (6.1) the maximum is taken over $1 \leq j \leq 3$ (the velocity components) and over all the nodes i of the mesh used. Observe that (6.1) implies that

$$\frac{||u_h^{n+1} - u_h^n||_\infty}{||u_h^n||_\infty} < 10^{-3} \tag{6.2}$$

Note however that (6.1) is a much more stringent condition than (6.2). The same computer programs were used to solve Dean's equations (1.13) - (1.17) for the range $96 \leq D \leq 3500$. The following slightly modified version of the fixed point scheme (see section 3.5) was found to accelerate the rate of convergence considerably

Given an initial approximation u_h^0, define

$$u_h^{n+\frac{1}{2}} = \Phi(u_h^n),$$

$$u_h^{n+1} = \lambda u_h^n + (1-\lambda)u_h^{n+\frac{1}{2}}$$

where $0 \leq \lambda < 1$ is an averaging parameter whose optimal value is determined by numerical experimentation. All the computations were carried out in double precision on a VAX - 11/750 computer.

6.2 Some comparisons

First of all it must be mentioned that the two schemes gave identical results for all the cases tested, but as expected, the least squares scheme proved to be much faster than the fixed point scheme of Chapter 3.

This must not be surprising since the fixed point scheme requires a huge number of matrix factorizations. The relative speed of the two schemes depends on the mesh size, for example, to compute the solutions of Dean's equations for $96 \leq D \leq 1000$ ($\Delta D = 100$) using MESH 24 (see

Figure 3), the fixed point scheme requires 39:04 minutes of CPU time, while the least squares scheme requires 57:45 minutes. Observe that in this case the fixed point scheme is faster than least-squares. However, to compute the flow at D = 2100 using MESH 96, the least-squares scheme requires 1:16:04 hours vs. 5:45:57 hours for the fixed point scheme.

We now turn to practical accuracy considerations.

In order to determine an adequate mesh size that gives good accuracy, three different mesh sizes were used to solve equations (1.14) - (1.17). Figure 3 shows the three meshes used. Table 1 shows the values of the maximum axial velocity u_{3max} at different Dean numbers, while table 2 shows the values of the axial velocity $u_3(0)$ at the center of the cross section

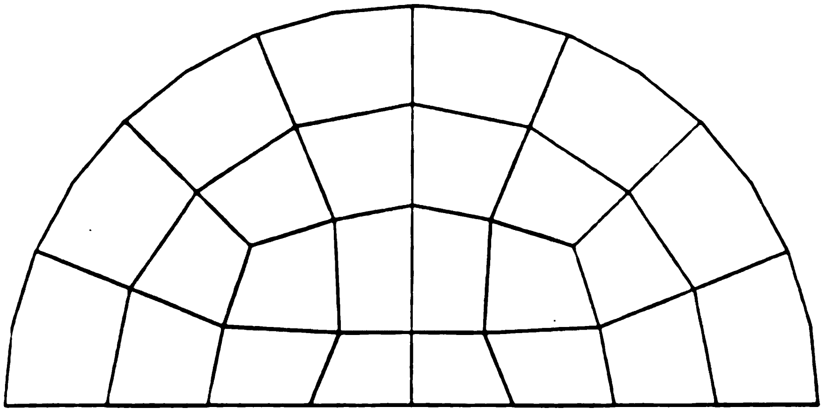

MESH 24
89 velocity nodes,33 pressure nodes,24 elements.

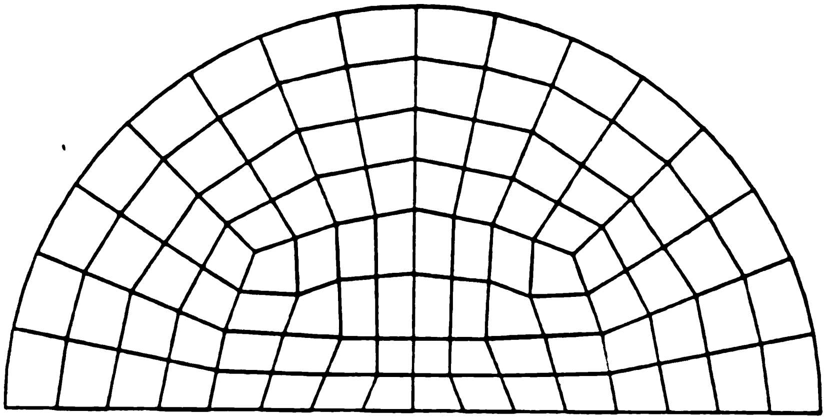

MESH 96
321 velocity nodes,113 pressure nodes,96 elements.

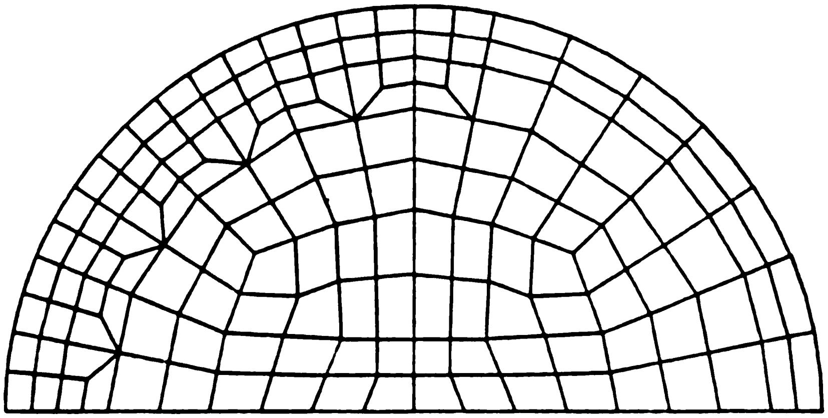

MESH 148
489 velocity nodes,171 pressure nodes,148 elements

Mesh configurations

Figure 3

D	MESH 24	MESH 96	MESH 148
96	23.30	23.35	———
500	84.26	83.77	83.72
1000	150.92	141.59	141.34
2000	——	238.64	237.48

Table 1: Variation of u_{3max} with mesh size

D	MESH 24	MESH 96	MESH 148
96	22.45	22.44	———
500	64.97	63.84	63.81
1000	103.45	99.54	99.32
2000	———	158.07	157.08

Table 2: Variation of $u_3(0)$ with mesh size

It is clear from tables 1 and 2 that the results obtained by MESH 148 and MESH 96 are in excellent agreement for $D \leq 2000$, thus indicating that either mesh is adequate for this range of the Dean number.

In tables 3 and 4, we compared the same quantities (u_{3max}, $u_3(0)$) obtained from the finest mesh (148) with the results of previous investigators. The tables indicate that our results are perfectly consistent with those of previous studies for $D \leq 2000$. The agreement is less than perfect for $D > 2000$ however. For this reason we restrict the results in section 6.3 to the range $D \leq 2000$, and restrict the values of R and ϵ accordingly, thus for $\epsilon = .1$ we make the restriction $R \leq 1118.03$, and for $\epsilon = .5$, $R \leq 500$.

We believe that if MESH 148 is refined all around the boundary (thus increasing the total number of velocity nodes to about 700 points), the flow in the entire laminar region can be accurately computed.

D	Present Study	Collins & Dennis (1975)	Dennis (1980)
500	83.72	83.69	83.67
605.72	96.53	96.53	——
1000	141.34	141.30	141.10
2000	237.48	236.50	——
3000	317.72	——	314.80
3500	354.72	351.40	——

Table 3: Comparison of u_{3max}

D	Present Study	Collins & Dennis (1975)	Dennis (1980)
500	63.81	63.70	63.78
605.72	72.10	——	——
1000	99.32	99.00	99.16
2000	157.08	154.70	——
3000	206.57	——	203.50
3500	230.31	224.70	——

Table 4: Comparison of $u_3(0)$

6.3 Results and discussion

The numerical results are summarized in Figures 4 - 11. Figures 4 - 7 show the contour lines of the axial velocity (u_3) and the stream function (ψ) of the secondary flow at R = 250 and R = 500 in the range $\frac{1}{10} \lesssim \epsilon \lesssim \frac{1}{2}$.

The stream function ψ is defined by

$$\text{(6.3)} \qquad \frac{\partial\psi}{\partial x_1} = - \sqrt{J}u_2, \ \frac{\partial\psi}{\partial x_2} = \sqrt{J}u_1 .$$

Clearly figures 4 - 7 show that the axial flow in diminished and the secondary currents become stronger as the curvature increaces.

In order to study the effect of curvature on the flow when the Dean number is fixed, we computed the solutions for D = 1000, D = 2000 in the range $0 \lesssim \epsilon \lesssim \frac{1}{2}$, and the results are shown in Figures 8 - 11. Observe that in Figures 8(a) - 11(a) (for $\epsilon = 0$), the results are in excellent qualitative agreement with those of Collins and Dennis (1975) and Dennis (1980).

Notice however that in this case the secondary flow is diffused as the curvature increases (see figures 9,11). The reason for this is that for a fixed value of D, the Reynolds number R decreases as ϵ increases (Recall that $D = 4R\sqrt{2\epsilon}$). We thus believe that from the physical point of view, the pair (R,ϵ) is a better set of parameters to study the motion than (D,ϵ), because when D is fixed, one cannot study the effect of curvature independently of the effect of the pressure gradient on the flow.

Table 5 shows the values of the flow ratio Q/Q_0 at R = 250, R = 500 as ϵ increased from $\frac{1}{10}$ to $\frac{1}{2}$, where Q_0 is the flow rate in the straight pipe at the same Reynolds number.

In table 6, we give the values of the flow ratio Q/Q_D for $D = 1000$, $D = 2000$ and the same range of values of ϵ, where now Q_D is the flow rate in the limit of zero curvature at the same Dean number.

Tables 5 and 6 show that when R is fixed, the flow ratio Q/Q_0 decreases rapidly with the curvature ratio, and that the variation of Q/Q_D with ϵ is minimal. Thus for a fixed Dean number, curvature has virtually no effect on the flow rate for practical values of ϵ. One must keep in mind however that for a fixed Dean number D, the curvature ratio ϵ cannot be increased without decreasing the pressure gradient, and these two competing factors seem to stablize the resistence of the tube (which should increase with increasing values of R and ϵ), and this is what we believe causes the flow ratio Q/Q_D to be almost constant.

ϵ	$R = 250$	$R = 500$
.1	0.748179	0.648668
.2	0.685238	0.585044
.3	0.645136	0.545185
.4	0.615091	0.516832
.5	0.591105	0.494718

Table 5: The flow ratio Q/Q_0

ϵ	$D = 1000$	$D = 2000$
.1	0.978992	0.970511
.2	0.959563	0.950805
.3	0.942704	0.933770
.4	0.928089	0.919073
.5	0.915433	0.906423

Table 6: The flow ratio Q/Q_D

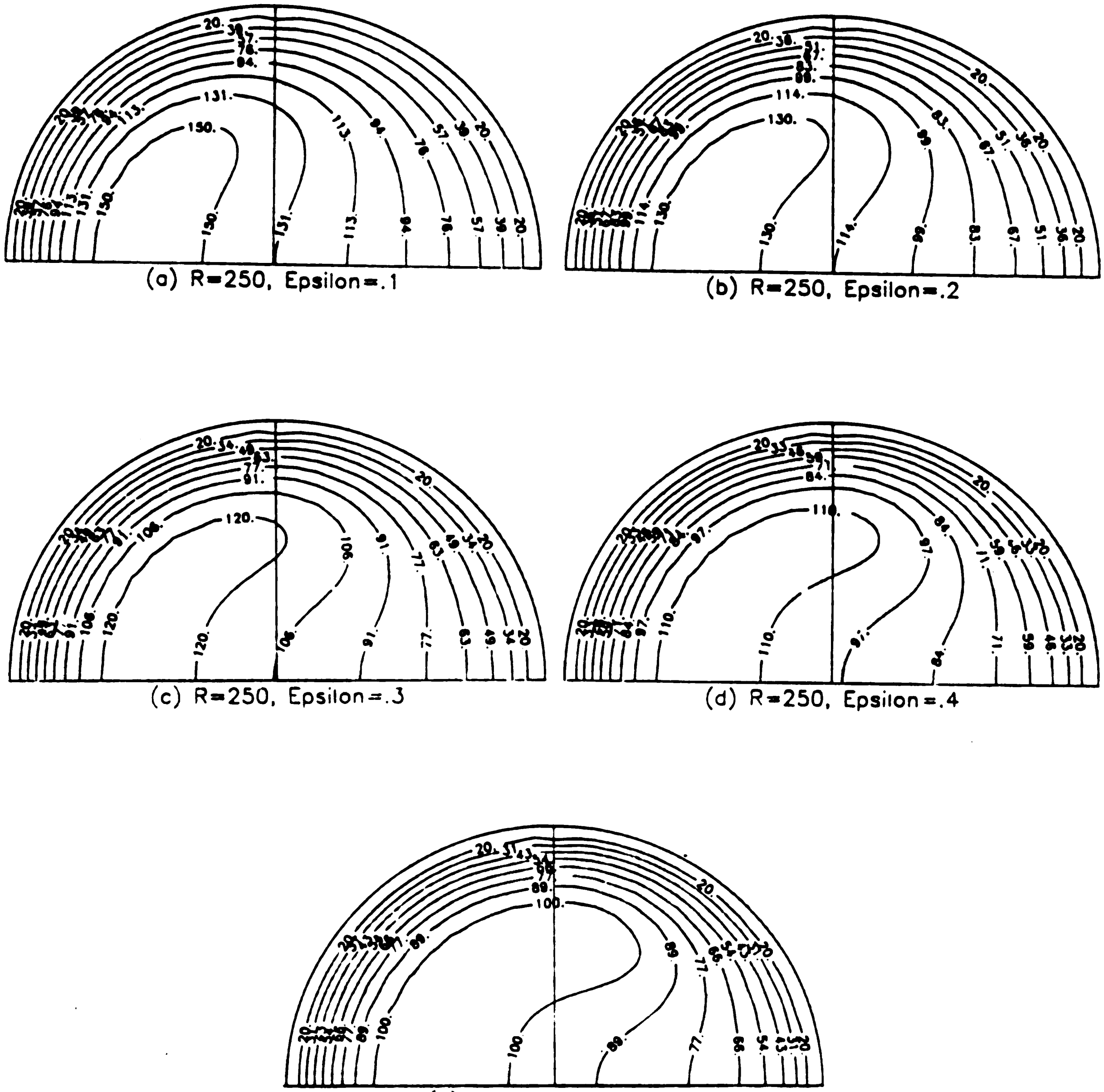

(a) R=250, Epsilon=.1

(b) R=250, Epsilon=.2

(c) R=250, Epsilon=.3

(d) R=250, Epsilon=.4

(e) R=250, Epsilon=.5

Contour lines of axial velocity at R=250

Figure 4

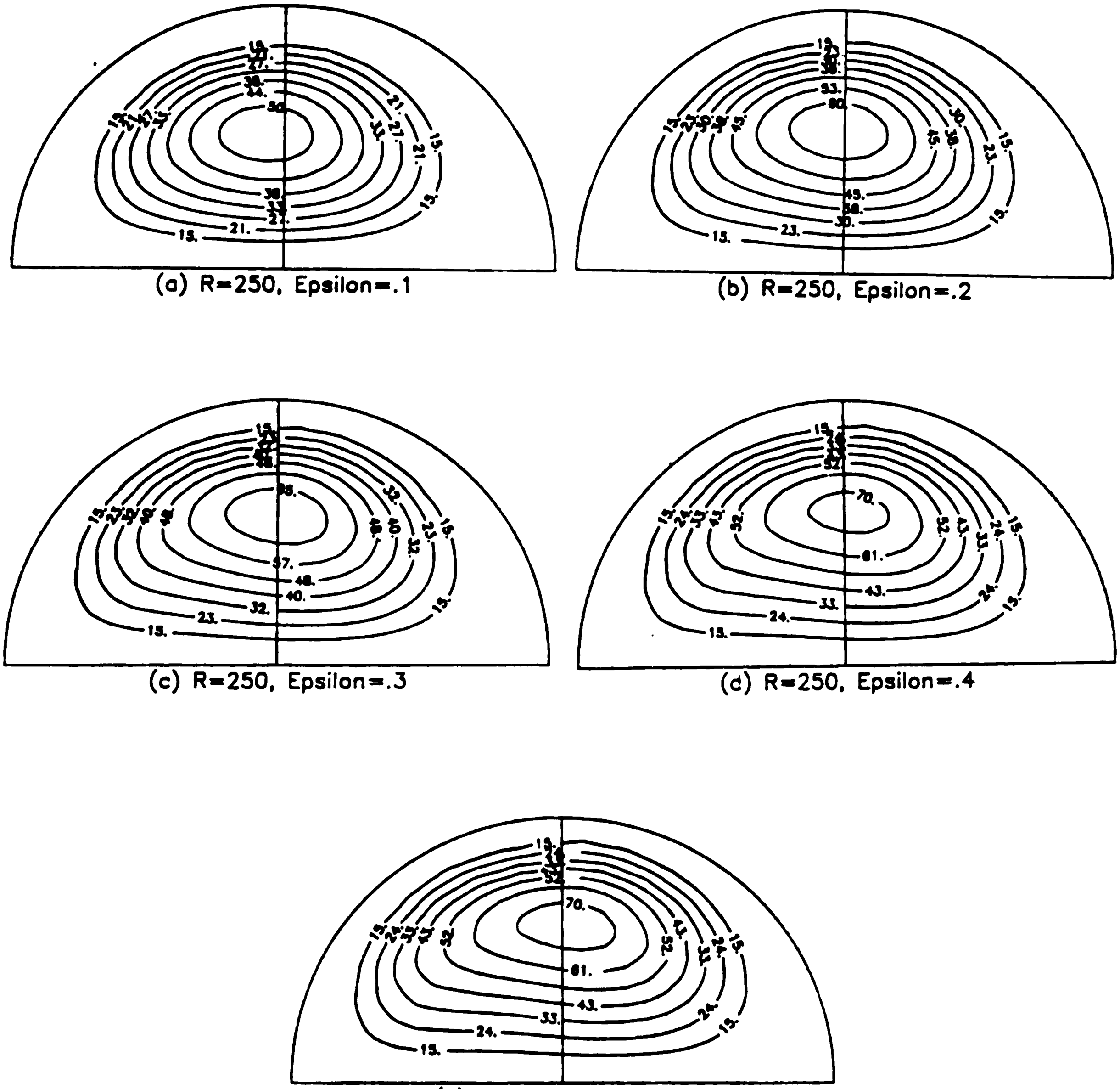

(a) R=250, Epsilon=.1

(b) R=250, Epsilon=.2

(c) R=250, Epsilon=.3

(d) R=250, Epsilon=.4

(e) R=250, Epsilon=.5

Secondary flow stream lines at R=250
Values shown are magnified 10 times

Figure 5

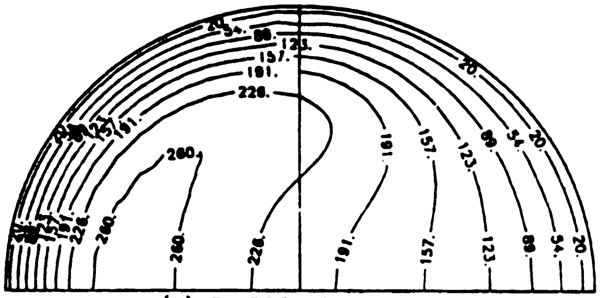

(a) R=500, Epsilon=.1

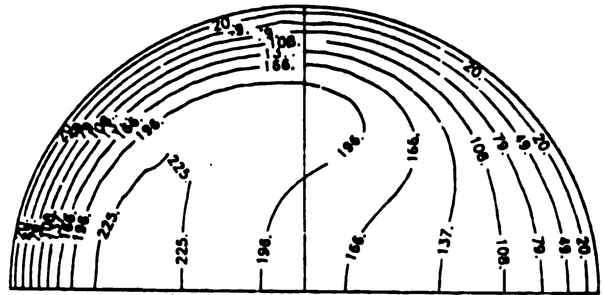

(b) R=500, Epsilon=.2

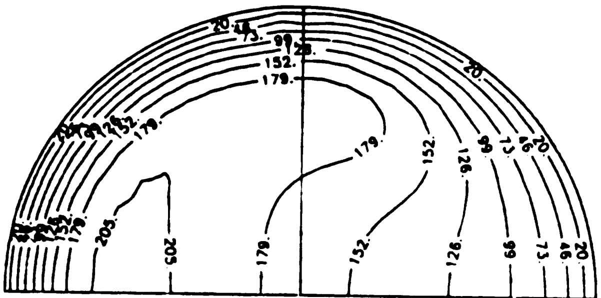

(c) R=500, Epsilon=.3

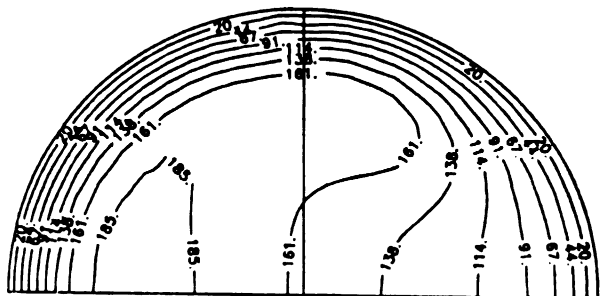

(d) R=500, Epsilon=.4

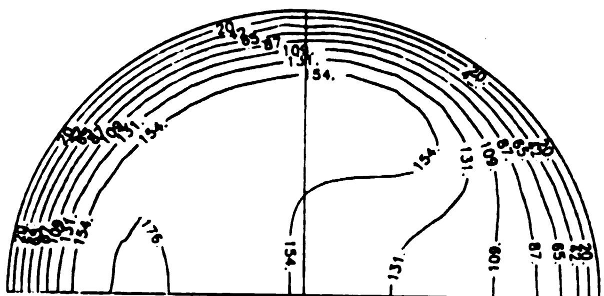

(e) R=500, Epsilon=.5

Contour lines of axial velocity at R=500

Figure 6

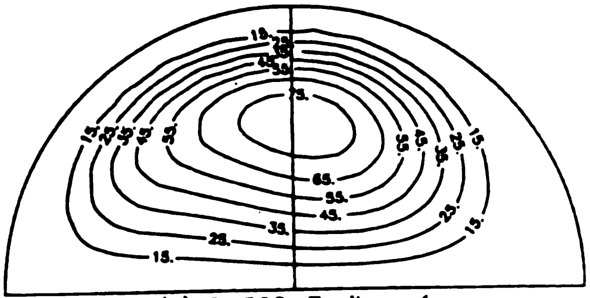

(a) R=500, Epsilon=.1

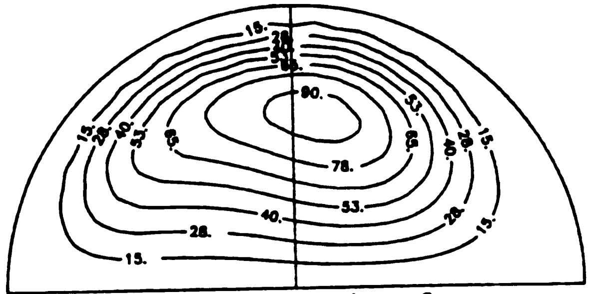

(b) R=500, Epsilon=.2

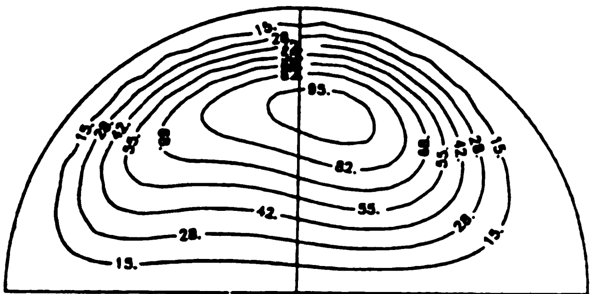

(c) R=500, Epsilon=.3

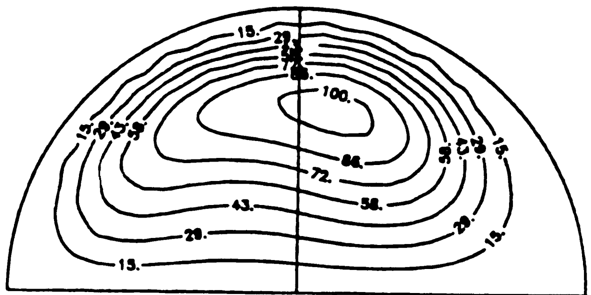

(d) R=500, Epsilon=.4

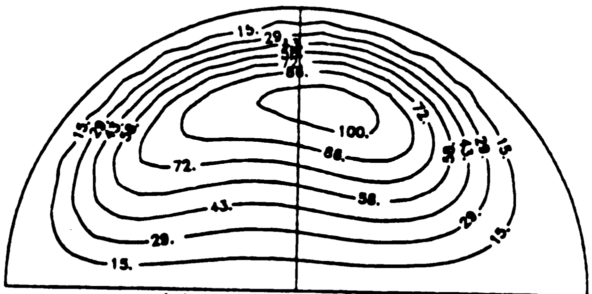

(e) R=500, Epsilon=.5

Secondary flow stream lines at R=500
Values shown are magnified 10 times

Figure 7

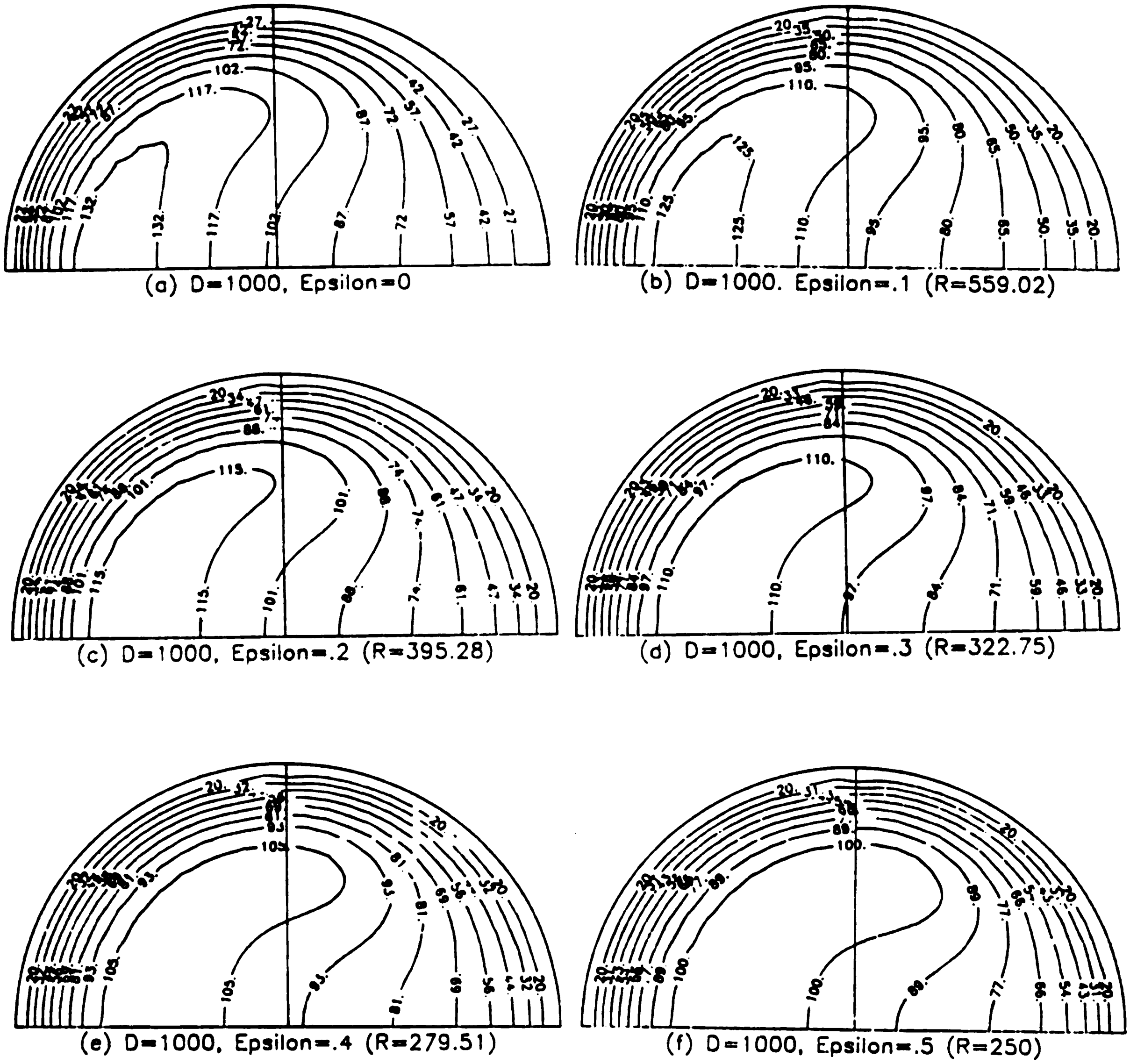

(a) D=1000, Epsilon=0

(b) D=1000. Epsilon=.1 (R=559.02)

(c) D=1000, Epsilon=.2 (R=395.28)

(d) D=1000, Epsilon=.3 (R=322.75)

(e) D=1000, Epsilon=.4 (R=279.51)

(f) D=1000, Epsilon=.5 (R=250)

Contour lines of axial velocity at D=1000

Figure 8

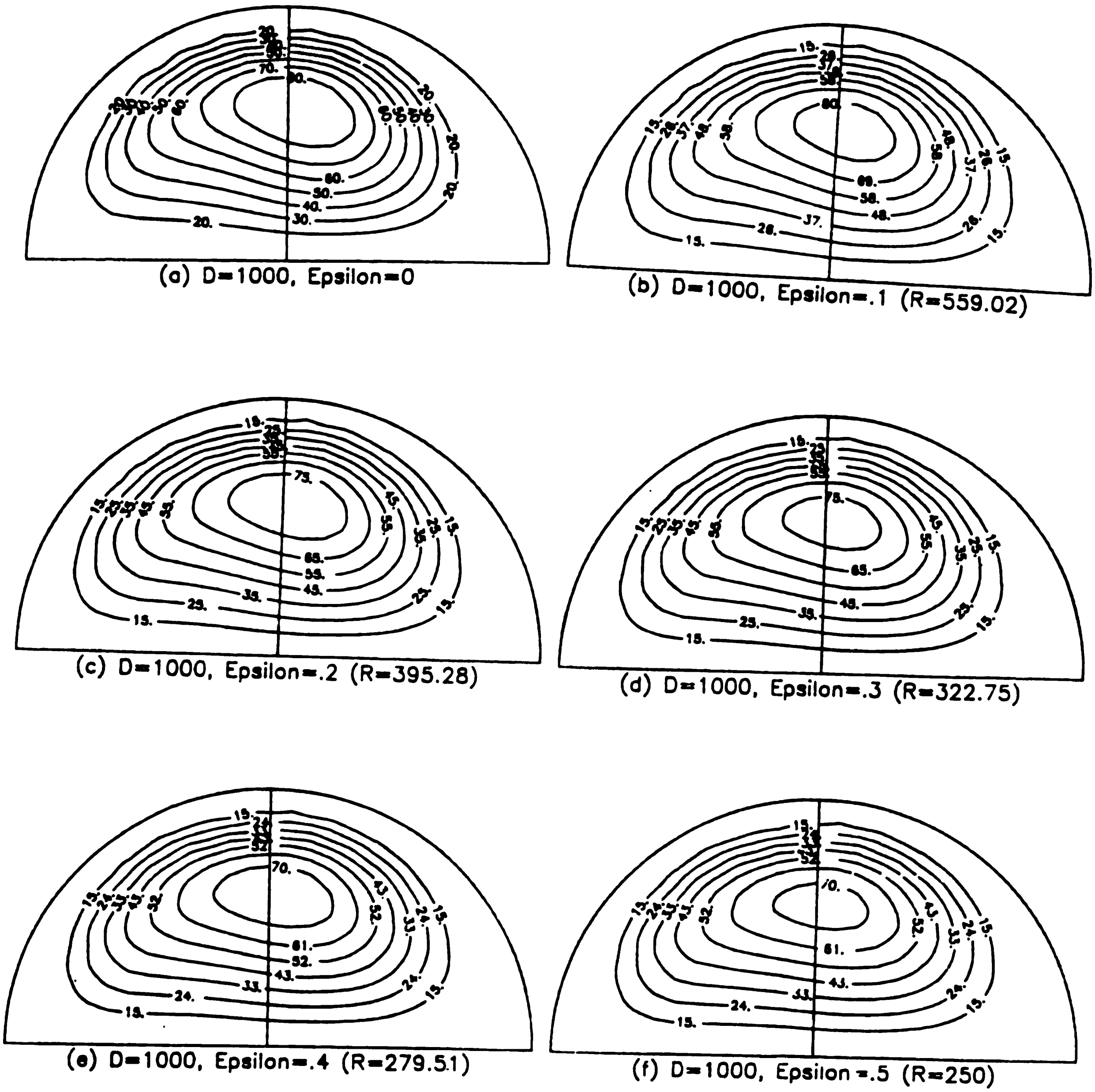

Secondary flow stream lines at D=1000.
Values shown are magnified 10 times

Figure 9

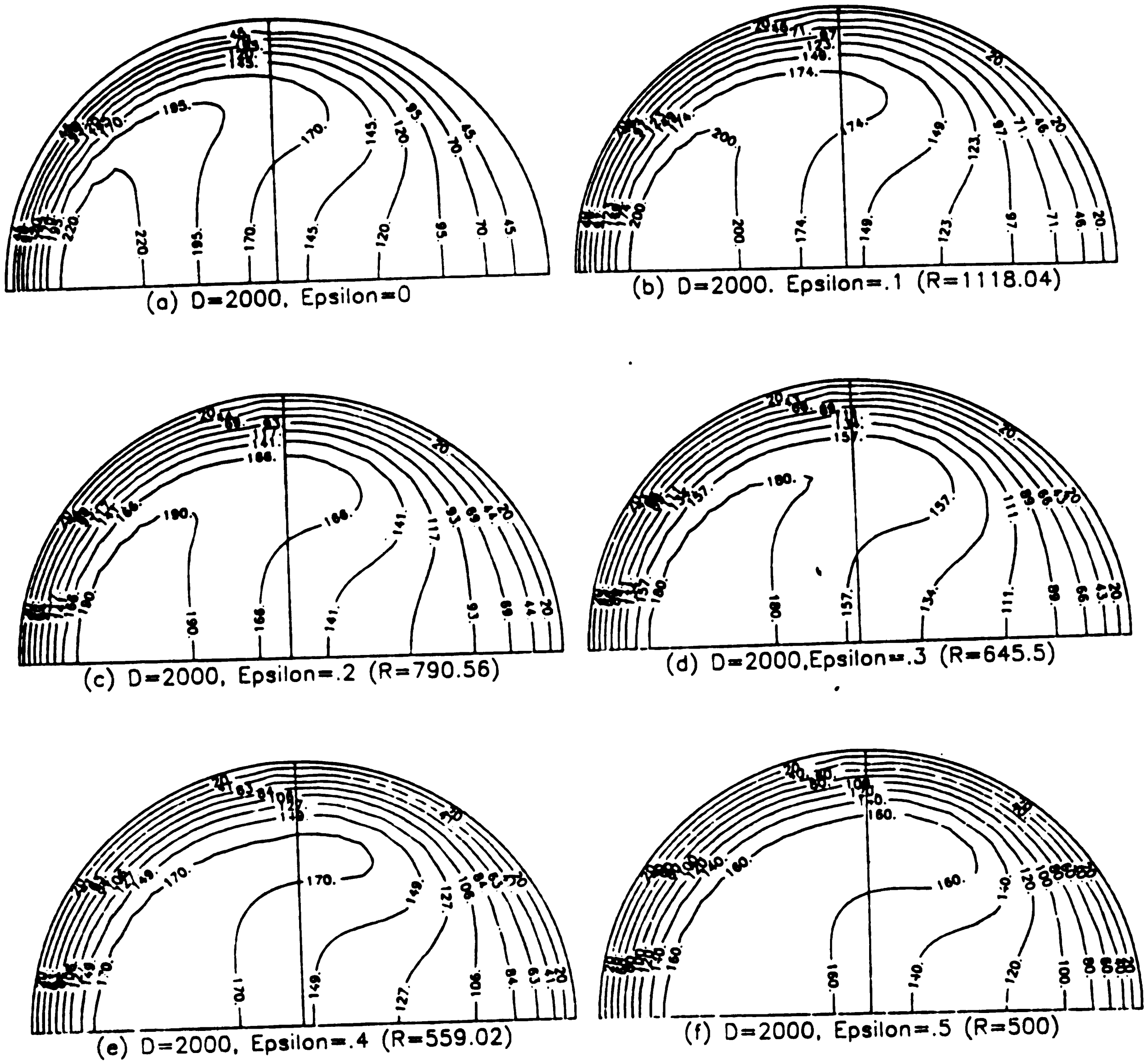

Contuor lines of axial velocity at D=2000

Figure 10

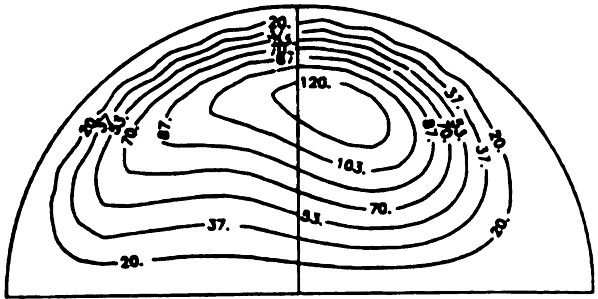

(a) D=2000, Epsilon=0

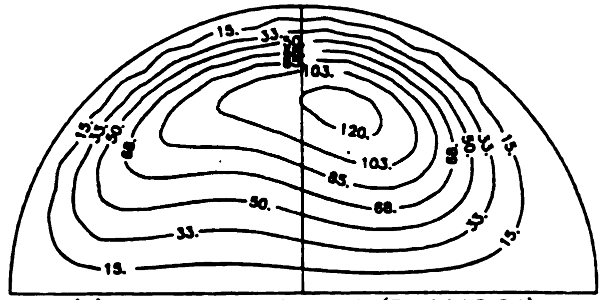

(b) D=2000, Epsilon=.1 (R=1118.04)

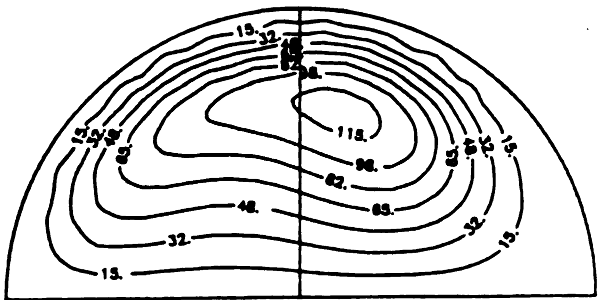

(c) D=2000, Epsilon=.2 (R=790.56)

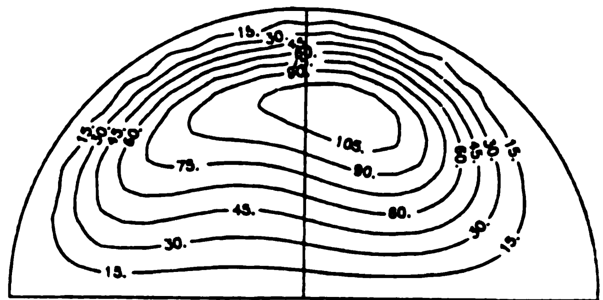

(d) D=2000, Epsilon=.3 (R=645.5)

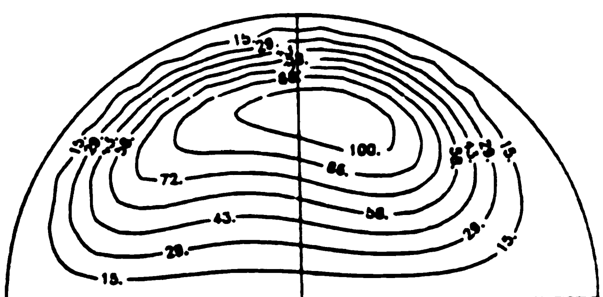

(e) D=2000, Epsilon=.4 (R=559.02)

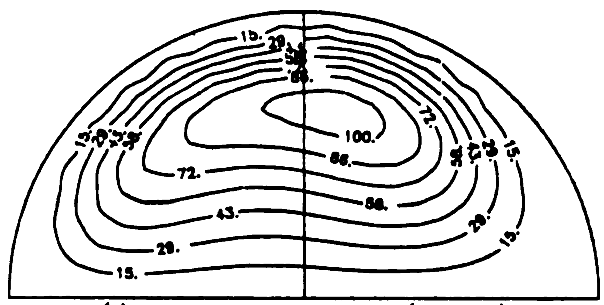

(f) D=2000, Epsilon=.5 (R=500)

Secondary flow stream lines at D=2000
Values shown are magnified 10 times

Figure 11

7.1 Introduction and formulation

The primary aim of this chapter is to give another example to demonstrate the fact that our solution procedure applies to duct flows in cross sections other than the circle.

Here we present a perturbation solution for the flow in a toroidal pipe of elliptic cross section. Results and comparisons with numerical solutions are given in the next section.

Consider the flow in a toroidal pipe whose cross section is an ellipse with axes 2a, 2b where one of the axes makes an angle α with the normal **N** of the center line of the tube. The geometry is shown in Figure 12.

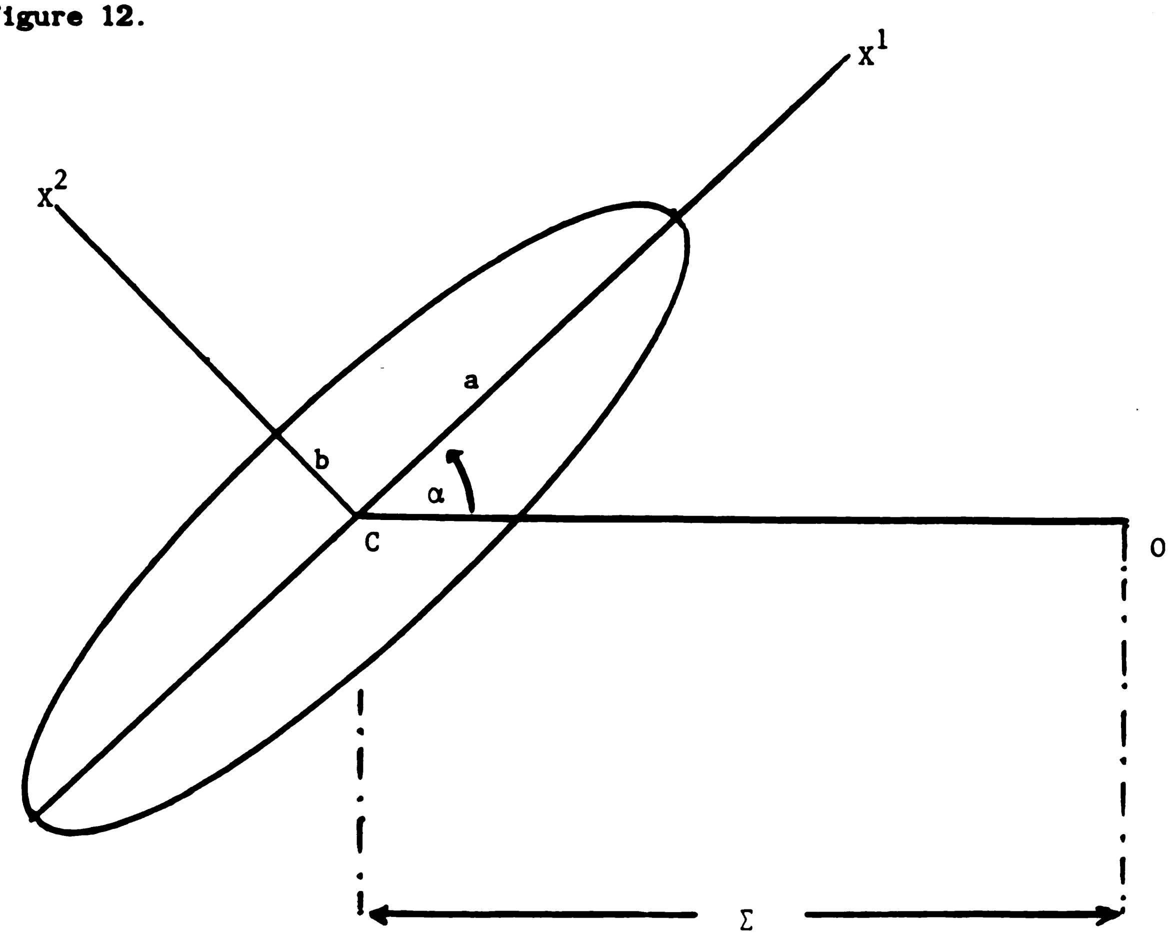

Geometry and coordinate system for elliptic cross section

Figure 12

As was done in chapter 1, it can be shown that the dimensionless momentum equations are

$$(7.1)\quad \left(u\frac{\partial}{\partial x} + v\frac{\partial}{\partial y}\right)u + \frac{\beta\epsilon w^2}{\sqrt{G}} = -\frac{\partial p}{\partial x} + \Delta u - \frac{\epsilon}{\sqrt{G}}\left(\beta\frac{\partial}{\partial x} - \delta\frac{\partial}{\partial y}\right)u - \frac{\beta\epsilon^2}{G}(\beta u - \delta v)$$

$$(7.2)\quad \left(u\frac{\partial}{\partial x} + v\frac{\partial}{\partial y}\right)v - \frac{\delta\epsilon w^2}{\sqrt{G}} = -\frac{\partial p}{\partial y} + \Delta u - \frac{\epsilon}{\sqrt{G}}\left(\beta\frac{\partial}{\partial x} - \delta\frac{\partial}{\partial y}\right)v + \frac{\delta\epsilon^2}{G}(\beta u - \delta v)$$

$$(7.3)\quad \left(u\frac{\partial}{\partial x} + v\frac{\partial}{\partial y}\right)\left(\frac{w}{\sqrt{G}}\right) - \frac{2\epsilon w}{G}(\beta u - \delta v) = \frac{4R}{G} + \Delta\left(\frac{w}{\sqrt{G}}\right) - \frac{3\epsilon}{\sqrt{G}}\left(\beta\frac{\partial}{\partial x} - \delta\frac{\partial}{\partial y}\right)\left(\frac{w}{\sqrt{G}}\right)$$

and the continuity equation

$$(7.4)\qquad \frac{\partial}{\partial x}(u\sqrt{G}) + \frac{\partial}{\partial y}(v\sqrt{G}) = 0$$

Where u,v are the dimensionless velocity components in the directions X^1, X^2 and w is the dimensionless axial velocity. In equations (7.1) - (7.4), $x = X^1/b$, $y = X^2/b$ are the normalized independent variables, $\beta = \cos\alpha$, $\delta = \sin\alpha$, $\epsilon = b/\Sigma$, $G = (1-\epsilon\beta x + \epsilon\delta y)^2$ and $R = \dfrac{-b^3}{4\rho\upsilon^2}\dfrac{\partial P}{\partial X^3}$ is the Reynolds number, where $\dfrac{\partial P}{\partial X^3}$ is the pressure gradient. The boundary conditions are

$$u\Big|_\Gamma = v\Big|_\Gamma = w\Big|_\Gamma = 0,$$

where Γ is the boundary of the elliptic region $c\,x^2 + y^2 \leq 1$, and $c = b^2/a^2$ is the aspect ratio.

Observe that is we set $a = b$, $\alpha = 0$ (thus $c = 1$, $\beta = 1$, $\delta = 0$), equations (7.1) - (7.4) reduce to equations (1.5) - (1.8).

In addition to the assumptions of Chapter 1, we assume that $\epsilon << 1$ and $R = O(1)$. Define the stream function ψ by

$$(7.5) \qquad u = \frac{1}{\sqrt{G}} \frac{\partial \psi}{\partial y}, \quad v = \frac{-1}{\sqrt{G}} \frac{\partial \psi}{\partial x}$$

substituting (7.5) into (7.3) yields the equation

$$(7.6) \quad \Delta w = \frac{1}{\sqrt{G}} \frac{\partial(\psi, w)}{\partial(y,x)} + \frac{\epsilon}{\sqrt{G}} \left(\beta \frac{\partial}{\partial x} - \delta \frac{\partial}{\partial y}\right) w + \frac{\epsilon^2 w}{G} - \frac{4R}{\sqrt{G}} - \frac{\epsilon w}{G} \left(\beta \frac{\partial}{\partial y} + \delta \frac{\partial}{\partial x}\right)\psi$$

$$\text{where } \frac{\partial(\psi, w)}{\partial(y,x)} = \frac{\partial \psi}{\partial y} \frac{\partial w}{\partial x} - \frac{\partial \psi}{\partial x} \frac{\partial w}{\partial y}$$

Eliminating p from (7.1) and (7.2) by cross differentiation, and keeping terms only up to $O(\epsilon^2)$ we obtain

$$(7.7) \quad \Delta^2 \psi = \frac{1}{\sqrt{G}} \frac{\partial(\psi, \Delta\psi)}{\partial(y,x)} + \epsilon\left(\beta \frac{\partial}{\partial y} + \delta \frac{\partial}{\partial x}\right) w^2 - \frac{2\epsilon}{\sqrt{G}} \left(\beta \frac{\partial}{\partial x} - \delta \frac{\partial}{\partial y}\right)(\Delta\psi)$$

Our discussion for obtaining a perturbation solution of (7.6) and (7.7) will be brief since our formulation and solution procedure is very similar to that of Srivastava (1980).

The axial velocity w and the stream function ψ are perturbed about $\epsilon = 0$

$$(7.8) \qquad w = w_0 + \epsilon w_1 + \epsilon^2 w_2 + \dots$$

$$(7.9) \qquad \psi = \epsilon \psi_1 + \epsilon^2 \psi_2 + \dots$$

Substituting (7.8), (7.9) into (7.6), (7.7) we obtain the following obtain the of linear equations upon comparing the coefficients of different powers of ϵ

$$\Delta w_0 = -4R \tag{7.10}$$

$$\Delta^2 \psi_1 = \left(\beta\frac{\partial}{\partial y} + \delta\frac{\partial}{\partial x}\right) w_0^2 \tag{7.11}$$

$$\Delta w_1 = \frac{\partial(\psi_1, w_0)}{\partial(y,x)} + \left(\beta\frac{\partial}{\partial x} - \delta\frac{\partial}{\partial y}\right) w_0 - 4R(\beta x - \delta y) \tag{7.12}$$

$$\Delta^2 \psi_2 = \frac{\partial(\psi_1, \Delta\psi_1)}{\partial(y,x)} + 2\left(\beta\frac{\partial}{\partial y} + \delta\frac{\partial}{\partial x}\right)(w_0 w_1) - 2\left(\beta\frac{\partial}{\partial x} - \delta\frac{\partial}{\partial y}\right)(\Delta\psi_1) \tag{7.13}$$

$$\begin{aligned} \Delta w_2 = {} & (\beta x - \delta y)\frac{\partial(\psi_1, w_0)}{\partial(y,x)} + \frac{\partial(\psi_1, w_1)}{\partial(y,x)} \\ & + \frac{\partial(\psi_2, w_0)}{\partial(y,x)} + (\beta x - \delta y)\left(\beta\frac{\partial}{\partial x} - \delta\frac{\partial}{\partial y}\right) w_0 \\ & + \left(\beta\frac{\partial}{\partial x} - \delta\frac{\partial}{\partial y}\right) w_1 - w_0\left(\beta\frac{\partial}{\partial y} + \delta\frac{\partial}{\partial x}\right)\psi_1 - 4R(\beta x - \delta y)^2 + w_0. \end{aligned} \tag{7.14}$$

Equations (7.10) - (7.14) are solved subject to the boundary conditions

$$w_j = \psi_j = 0, \quad \nabla\psi_j = 0 \quad \text{on the boundary}$$

$$cx^2 + y^2 = 1$$

The exact solutions of equations (7.10) - (7.14) can be computed in turn since in fact all the functions w_j, ψ_j are polynomials in x,y. The solution for (7.10) can be easily seen to be

$$w_o = KR(cx^2 + y^2 - 1), \qquad K = \frac{-2}{1+c} \tag{7.15}$$

Now (7.15) and (7.11) give the equation

$$\Delta^2\psi_1 = 4\, cK^2R^2\delta x(cx^2 + y^2 - 1) + 4K^2R^2\beta y(cx^2 + y^2 - 1)$$

whose solution is

$$\psi_1 = R^2\delta P_1(x,y,c) + R^2\beta P_2(x,y,c) \tag{7.16}$$

where for example

$$P_1 = x(p_{00} + p_{20}x^2 + p_{02}y^2)(cx^2 + y^2 - 1)^2$$

and the coefficients p_{00}, p_{20}, p_{02} are obtained by substituting (7.16) in (7.11) and comparing the coefficients. This leads to a 3×3 matrix equation for the coefficients p_{00}, p_{20}, p_{02}.

Solutions of equations (7.12) - (7.14) can be obtained similarly. Many more details can be found in Srivastava (1980).

It must be observed that, although the procedure for solving (7.10) - (7.14) is very simple in principle, the process of comparing coefficients and inverting matrices to obtain the coefficients of the (polynomial) solutions becomes impossible to do by hand as one proceeds to compute w_1, ψ_2, w_2. A rather lengthy computer program was written to carry out the calculation.

7.2 Results and discussion

We begin by giving the results for an elliptic region where $c = \frac{1}{4}$, thus the cross section is

$$\frac{x^2}{4} + y^2 \leq 1$$

Figures 13 - 15 show the first order stream lines ψ_1 / R^2 for $\alpha = 0$, $\alpha = \frac{\pi}{4}$, $\alpha = \frac{\pi}{2}$ respectively.

It must be mentioned here that the results of Srivastava (1980) can all be easily reproduced if we choose $\alpha = 0$ in our formulation.

All the comparisons given below are for the flow rate $Q = \int w$ (where the integral is taken over the elliptic region). From (7.8) we have

$$Q = \int w_0 + \epsilon \int w_1 + \epsilon^2 \int w_2.$$

It is easy to see that w_1 is an odd degree polynomial and therefore does not contribute to the flow rate, thus

$$Q = Q_0 + \epsilon^2 \int w_2.$$

where $Q_0 = \int w_0$ is the flow rate in the straight pipe.

It is easy to show that

$$w_2 = RD_1(x,y) + R^3 E_1(x,y) + R^5 F_1(x,y)$$

where D_1, E_1, F_1 are polynomials and R is the Reynolds numbers.

Now the flow ratio Q/Q_0 is given by

$$\frac{Q}{Q_0} = 1 + \epsilon^2(D + R^2E + R^4F) \tag{7.17}$$

where $D = \frac{R}{Q_0}\int D_1$, $E = \frac{R}{Q_0}\int E_1$, $F = \frac{R}{Q_0}\int F_1$ are constants that depend on β, δ and c.

It is worth mentioning here that the results given by Srivastava (1980) for the flow ratio coefficients D,E,F are completely erroneous. In table 7, we quoted Srivastava (1980) for the coefficients D,E,F for different values of c, and in table 8 we give the correct values of the same coefficients.

c	D	E	F
0.25	-1.7617875	-0.0037665	-0.00001032
0.50	-1.6960690	-0.0019303	-0.00000212
0.75	-0.0052929	-0.0010727	-0.00000083
0.98	0.0201415	-0.0006594	-0.00000038
1.0	0.0208331	-0.0006334	-0.00000036
1.0201	0.0213993	-0.0006085	-0.00000033
1.25	0.0223002	-0.0003923	-0.00000017

Table 7: Coefficients in Equation (7.17)

(Srivastava(1980))

c	D	E	F
0.25	0.419048	-0.003770	-0.00000386
0.50	0.133333	-0.001935	-0.00000188
0.75	0.053724	-0.001077	-0.00000083
0.98	0.022655	-0.000663	-0.00000039
1.0	0.020833	-0.000637	-0.00000037
1.0201	0.019102	-0.000612	-0.00000035
1.25	0.004678	-0.000395	-0.00000017

Table 8: Coefficients in Equation (7.17)

(Present Study)

Finally we employed the method of chapter 5 to generate numerical solutions of the problem with $c = \frac{1}{4}$, $\alpha = \frac{\pi}{4}$ for R = 6, R = 20, R = 50, and the flow ratio Q/Q_0 was computed for each R in the range $\frac{1}{10} \lesssim \epsilon \lesssim .45$.

The flow ratio Q/Q_0 was then calculated for the same values of R and ϵ using the asymptotic formula (7.17) and the two sets of results are summarized in Figures 16 - 18. As is obvious from Figure 16, the results are in excellent agreement at R = 6, but the asymptotic solution deviates considerably from the numerical solution as R increases. (Recall that the perturbation solution is valid under the assumptions that $\epsilon \ll 1$, $R = O(1)$)

Finally observe that at R = 6, the flow rate actually increases with increasing values of ϵ. In fact, for the given data ($c = \frac{1}{4}$, $\alpha = \frac{\pi}{4}$), equation (7.17) takes the form

$$Q/Q_0 = 1 + \epsilon^2(1.809925 - 0.033573R^2 - 0.000055R^4)$$

and the expression in brackets is positive for $R < \sqrt{49.8165} = 7.058$. The numerically computed values of Q/Q_0 reflect the same phenomenon (see Figure 16).

It must be mentioned that the same phenomenon (that Q/Q_0 increases with ϵ at low Reynolds numbers) was reported by Larrain and Bonilla (1970) for toroidal pipes of circular cross section, and was later confirmed by Wang (1981) who discovered that the same phenomenon occurs for helically coiled tubes at small values of ϵ and low Reynolds numbers.

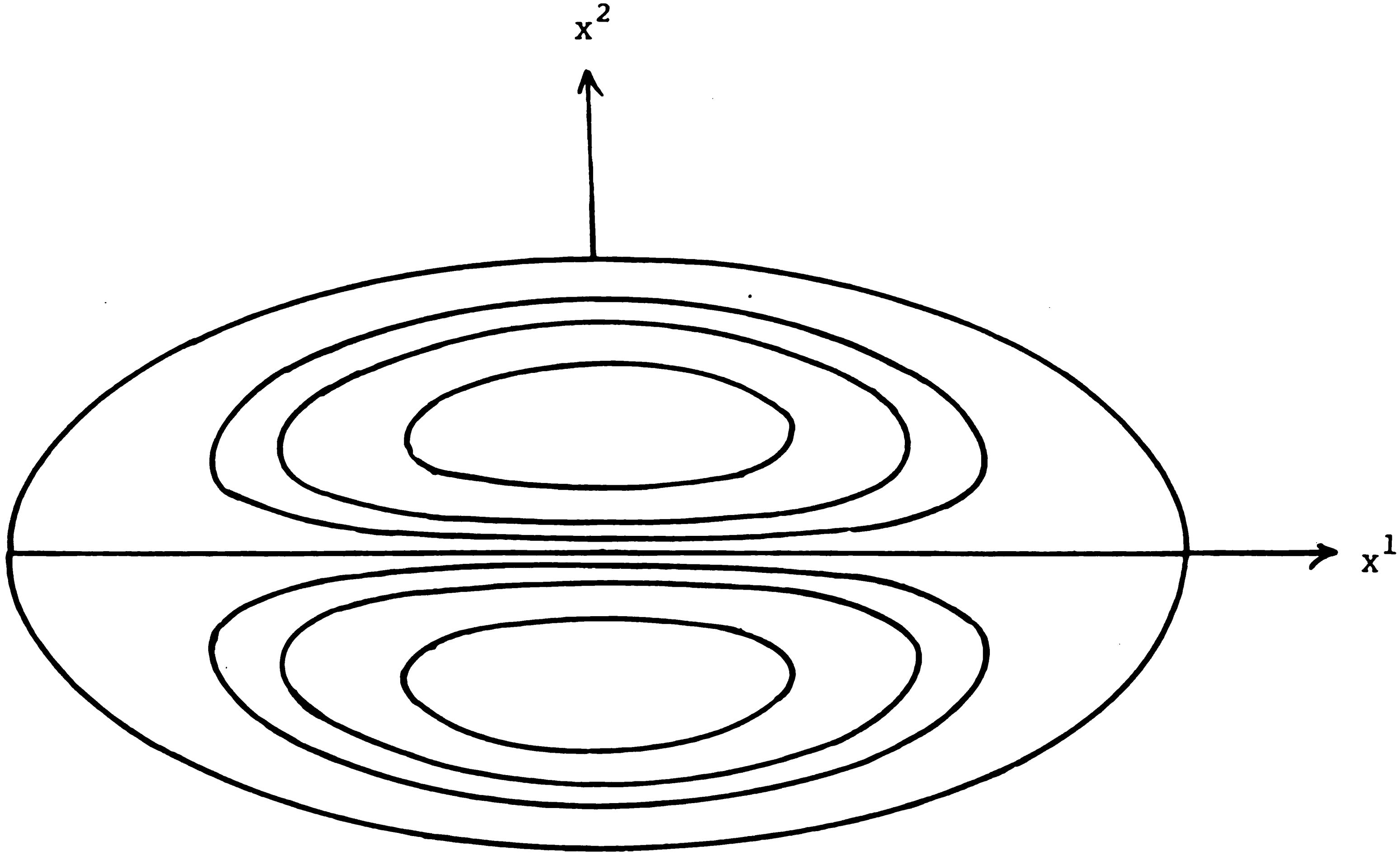

Stream lines for $\alpha = 0^{o}$ (Perturbation solution)

Figure 13

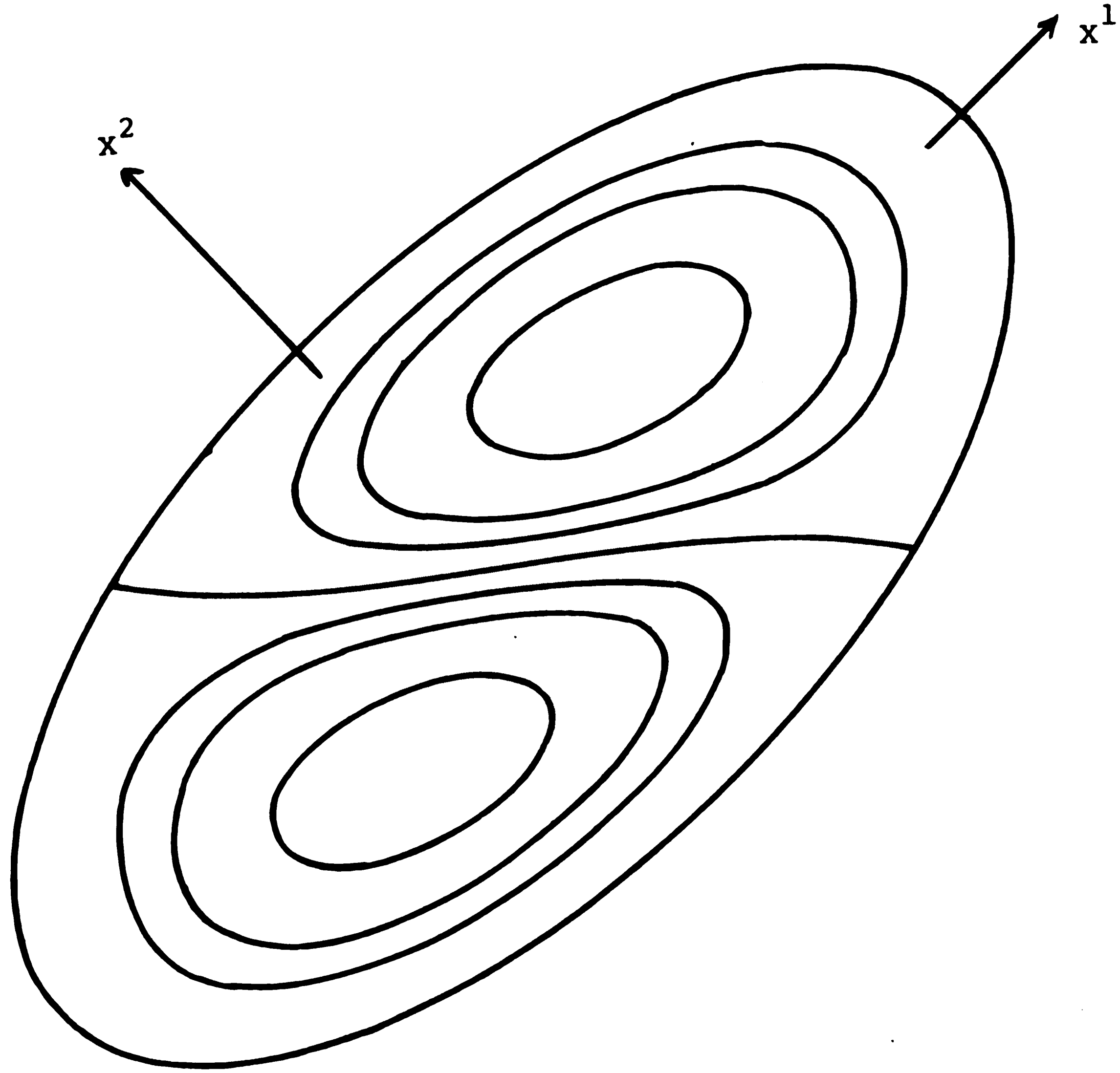

Stream lines for $\alpha = 45^{o}$ (perturbation solution)

Figure 14

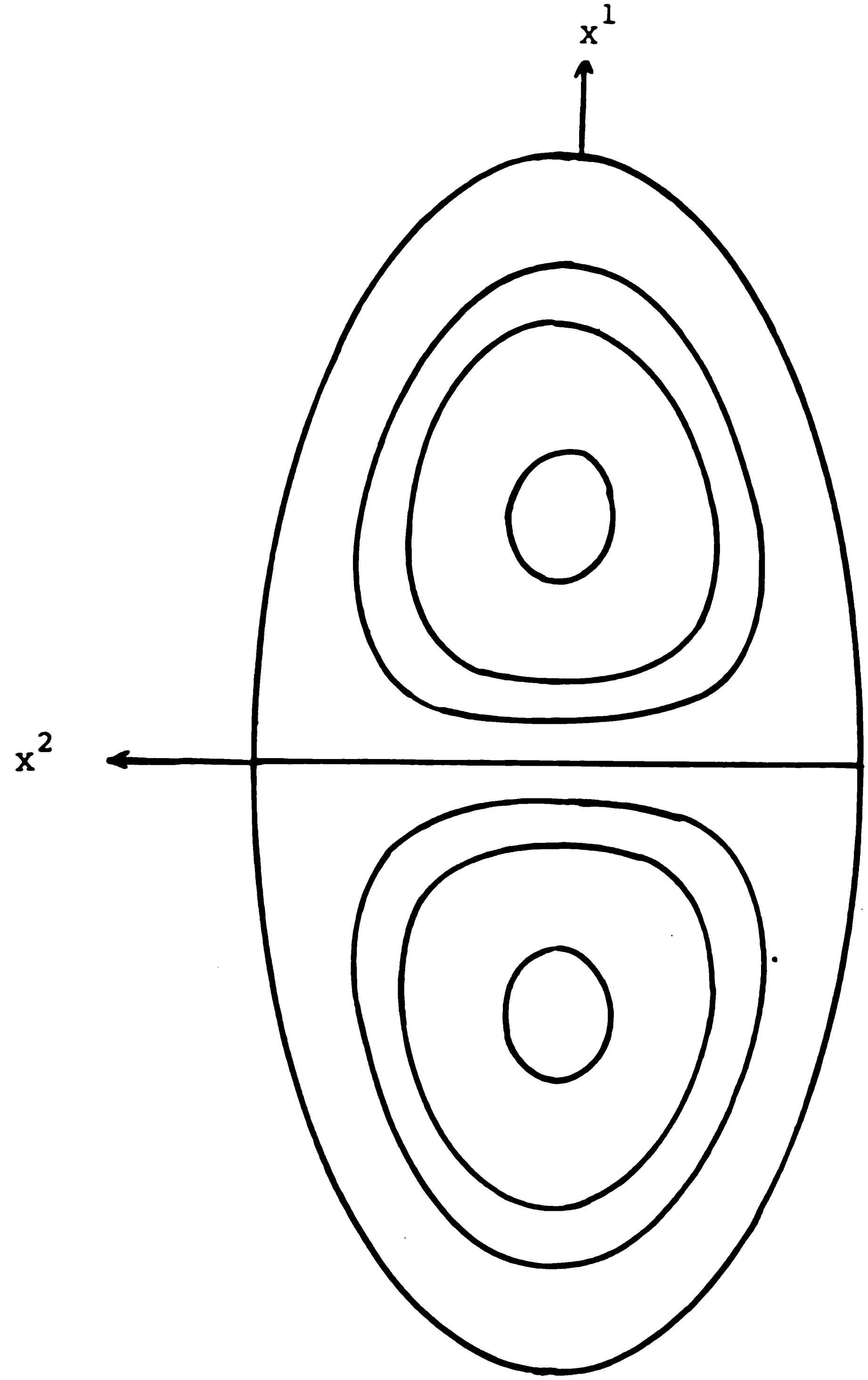

Stream lines for $\alpha = 90^{\circ}$ (Perturbation solution)

Figure 15

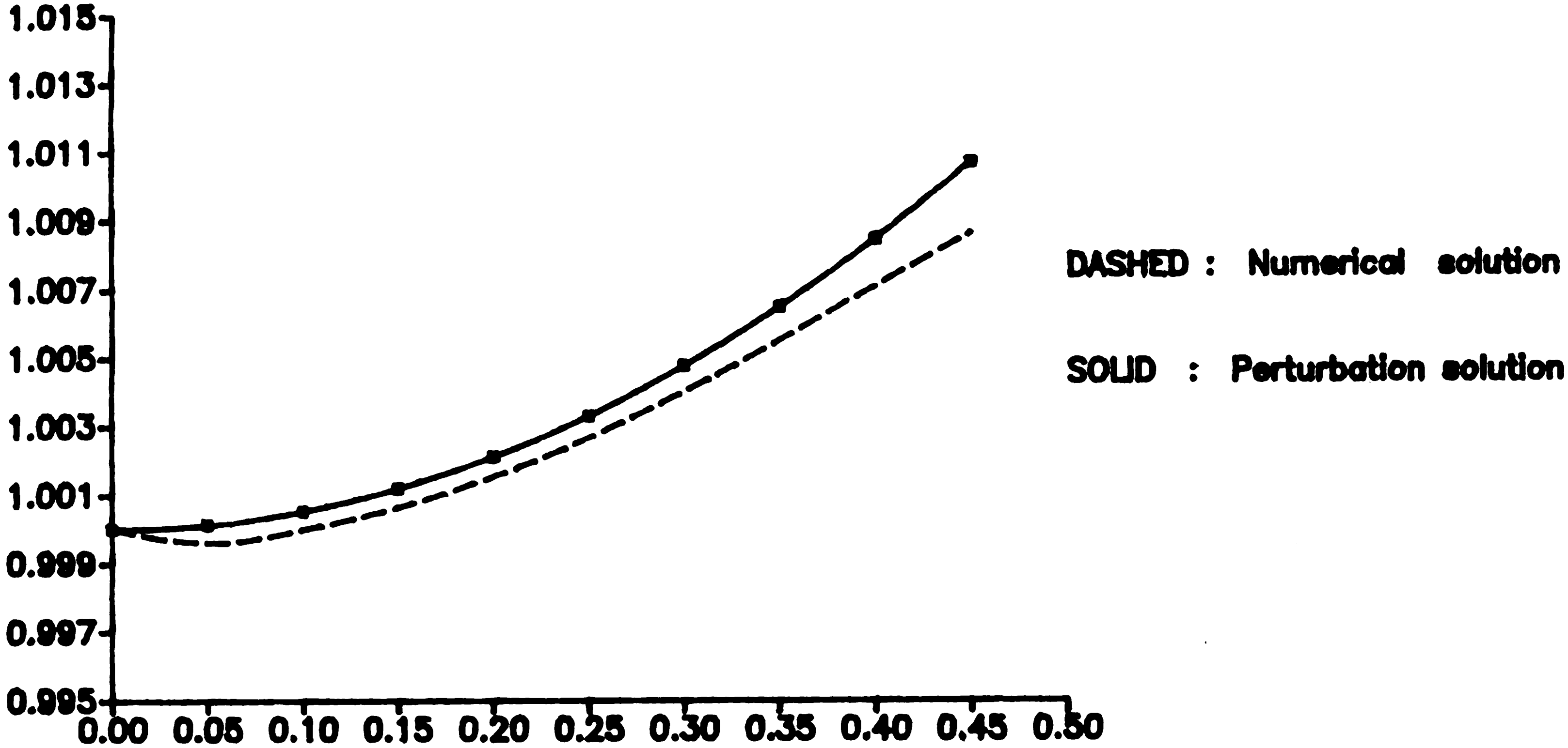

EFFECT OF CURVATURE ON FLOW RATIO
R=6.0

Figure 16

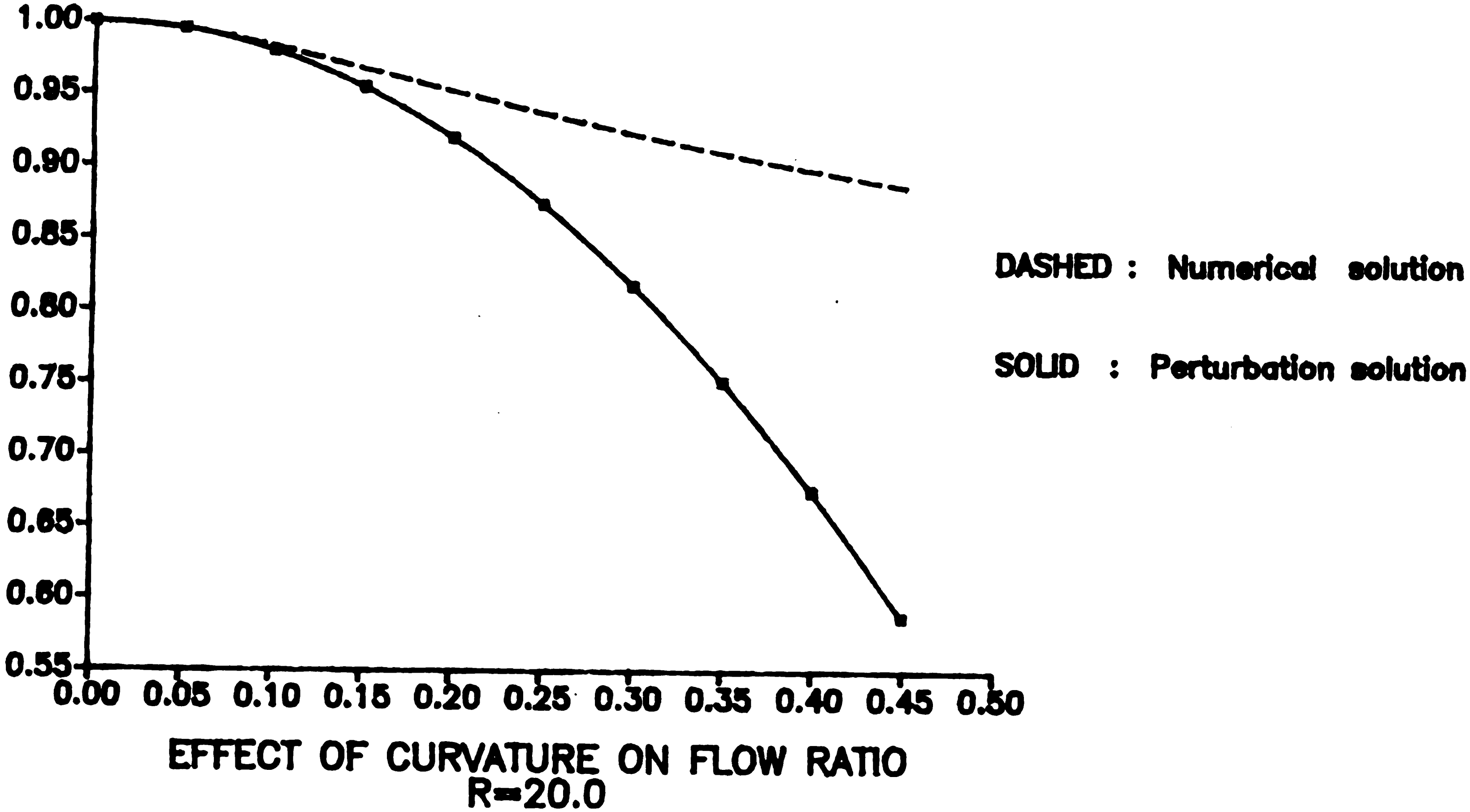
1.00
0.95
0.90
0.85
0.80
0.75
0.70
0.65
0.60
0.55
0.00 0.05 0.10 0.15 0.20 0.25 0.30 0.35 0.40 0.45 0.50
EFFECT OF CURVATURE ON FLOW RATIO
R=20.0
DASHED : Numerical solution
SOLID : Perturbation solution

Figure 17

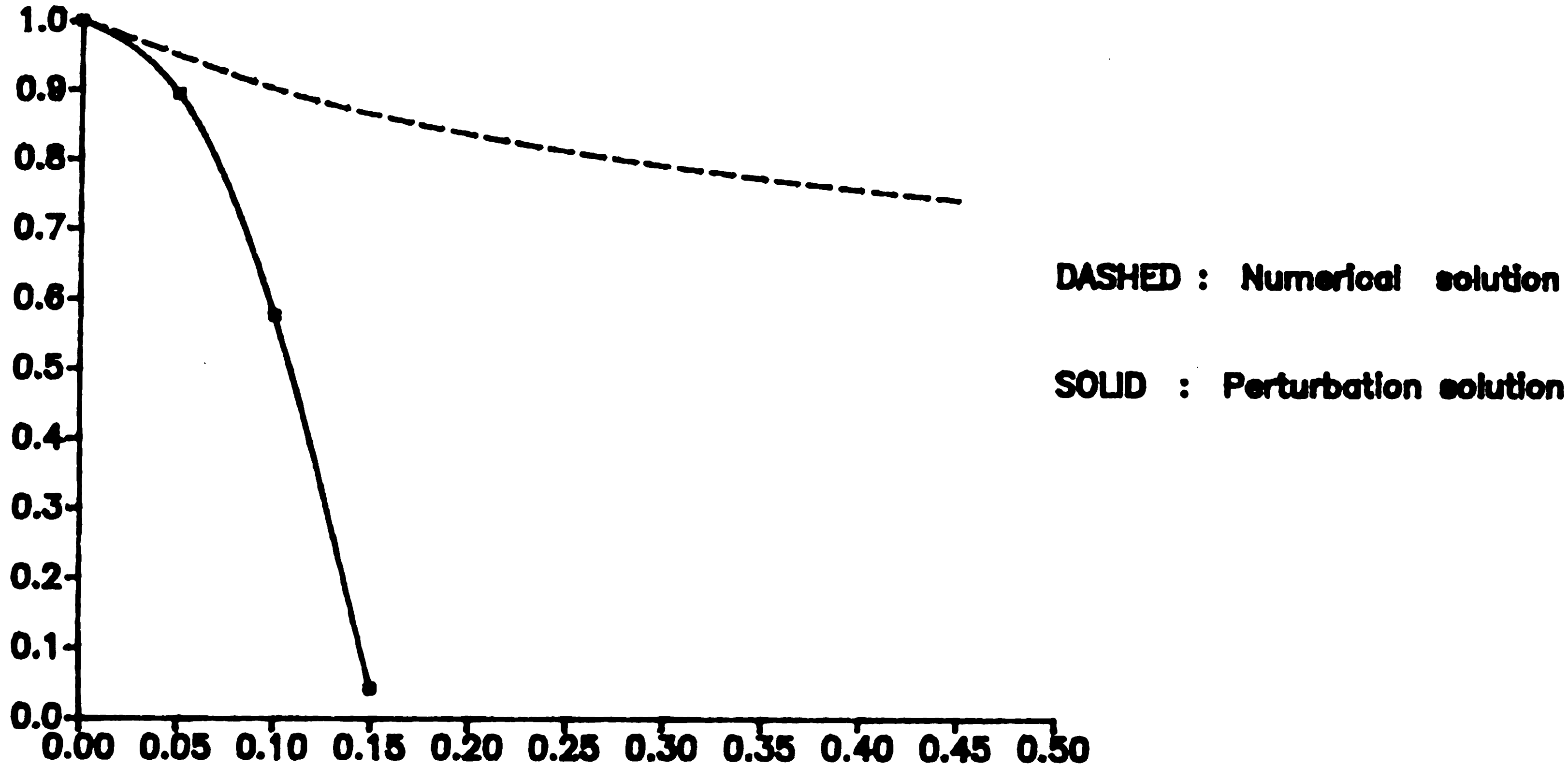

EFFECT OF CURVATURE ON FLOW RATIO
R=50.0

Figure 18

Appendix A

The covariant velocity components $V^i_{,jk}$

$$V^1_{,11} = \frac{\partial^2 U^1}{\partial (X^1)^2}$$

$$V^1_{,22} = \frac{\partial^2 U^1}{\partial (X^2)^2}$$

$$V^1_{,33} = - \kappa\sqrt{J}\,\frac{\partial U^1}{\partial X^1} - \kappa^2 U^1$$

$$V^2_{,11} = \frac{\partial^2 U^2}{\partial (X^1)^2}$$

$$V^2_{,22} = \frac{\partial^2 U^2}{\partial (X^2)^2}$$

$$V^2_{,33} = - \kappa\sqrt{J}\,\frac{\partial U^2}{\partial X^1}$$

$$V^3_{,11} = \frac{\partial^2}{\partial (X^1)^2}\left[\frac{U^3}{\sqrt{J}}\right] - \frac{2\kappa}{\sqrt{J}}\,\frac{\partial}{\partial X^1}\left[\frac{U^3}{\sqrt{J}}\right]$$

$$V^3_{,22} = \frac{\partial^2}{\partial (X^2)^2}\left[\frac{U^3}{\sqrt{J}}\right]$$

$$V^2_{,33} = - \kappa\sqrt{J}\,\frac{\partial}{\partial X^1}\left[\frac{U^3}{\sqrt{J}}\right]$$

Appendix B

In this appendix we outline the method we used to solve the matrix equation

$$(3.23) \qquad \begin{bmatrix} A & 0 & (D^1)^T & 0 \\ 0 & A^1 & (D^2)^T & 0 \\ D^1 & D^2 & 0 & 0 \\ 0 & 0 & 0 & A \end{bmatrix} \begin{bmatrix} U_1 \\ U_2 \\ P \\ U_3 \end{bmatrix} = \begin{bmatrix} G_1 \\ G_2 \\ 0 \\ G_3 \end{bmatrix}$$

The reader is reminded that the matrices A and A^1 are symmetric, positive definite, and banded, thus they were computed, stored compactly and then factored in place using LINPACK routine DPBFA which carries out the Choleski decomposition of a symmetric positve definite banded matrix.

Observe that (3.23) is a block diagonal system,thus U_3 can be computed separately by

$$(B.1) \qquad U_3 = A^{-1}G_3$$

where $A^{-1}G_3$ is found by using the LINPACK routine DPBSL which carries out the back substitution step since the Choleski decomposition of A is now available.

The discrete velocity vectors U_1 , U_2. and the discrete pressure P were computed as follows : system (3.23) is equivalent to the equations

$$(B.2) \qquad AU + D^TP = G,$$

$$(B.3) \qquad DU = 0$$

where $D = (D^1, D^2)$, $A = \begin{bmatrix} A & 0 \\ 0 & A^1 \end{bmatrix}$, $G = \begin{bmatrix} G_1 \\ G_2 \end{bmatrix}$, $U = \begin{bmatrix} U^1 \\ U^2 \end{bmatrix}$.

observe that

$$P = (DA^{-1}D^T)^{-1}\, D\, A^{-1}\, G, \tag{B.4}$$

and that once P is known, $U = \begin{bmatrix} U_1 \\ U_2 \end{bmatrix}$ can be computed

directly from (B.2) since

$$U = A^{-1}(G - D^T P). \tag{B.5}$$

The matrix $DA^{-1}D^T$ was computed by applying the back substitution routine as many times as D^T has columns, and then premultiplying the result $A^{-1}D^T$ by D. Observe that computing $DA^{-1}D^T$ requires many back substitutions for A, and then a matrix multiplication, but the effort taken to accopmlish this is well justified since several thousand solutions of (3.23) are required.

Since $DA^{-1}D^T$ is symmetric and positive definite (it is a full matrix however) , its Choleski decomposition was found by applying the LINPACK routine DPPFA, which factors $DA^{-1}D^T$ in place, and stores it compactly since it is symmetric.

Now each time we solve equation (3.23), we proceed as follows:

(i) Find U_3 by (B.1)

(ii) Find P by (B.4)

(iii) Find $U = \begin{bmatrix} U^1 \\ U^2 \end{bmatrix}$ by (B.5)

LIST OF REFERENCES

LIST OF REFERENCES

[1] Bercovier,M. and Pironneau,O. (1979) Error estimates for finite element method solution of the Stokes problem in primitive variables. Numer. Math. 33 : 211-224.

[2] Berger,S.A. , Talbot,L. and Yao,L.S. (1983) Flow in curved pipes. Ann. Rev. fluid Mech. 15 : 461-512.

[3] Carey,G.F. and Oden,J.T. (1986) Finite elements. The Texas finite element series. Vols. 4,6. Prentice-Hall.

[4] Ciarlet,P. (1978) The finite element method for elliptic equations. Studies in mathematics and its applications. Vol.4. North-Holland.

[5] Collins,W.M. and Dennis,S.C.R. (1975) The steady motion of a viscous fluid in a curved tube. Q.J. Mech. Appl. Math. 28 : 133-156.

[6] Collins, W.M. and Dennis, S.C.R. (1976) Steady flow in a curved tube of triangular cross section. Proc. R. Soc. London. Ser.A. 352 : 189-211.

[7] Cuming,H.G. (1952) The secondary flow in curved pipes. Aeronaut. Res.Counc. Rep. Mem. No. 2880.

[8] Dennis,S.C.R. (1980) Calculation of the steady flow through a curved tube using a new finite-difference method. J. Fluid Mech. 99 :449-467.

[9] Dennis,S.C.R. and Ng,M. (1982) Dual solutions for steady laminar flow through a curved tube. Q.J. Mech. Appl. Math. 35 : 305-324.

[10] Girault,V. and Raviart,P.A. (1979) Finite element approximation of the Navier-Stokes equations. Springer, Lecture notes in mathematics No. 749.

[11] Glowinski,R. (1984) Numerical methods for nonlinear variational problems. Springer series in computational physics.

[12] Glowinski,R. and Pironneau O. (1979) On a mixed finite element approximation of the Stokes problem. (I) Convergence of the approximate solutions. Numer. Math. 33 : 397-424.

[13] Greenspan,A.D. (1973) Secondary flow in a curved tube. J. Fluid Mech. 57 : 167-176.

[14] Hood,P. and Taylor,C. (1973) A numerical solution of the Navier-Stokes equations using the finite element technique. Computers and fluids. 1 : 73-100.

[15] Joseph,B. , Smith,E.P. and Adler,R.J. (1975) Numerical treatment of laminar flow in helically coiled tubes of square cross-sections. Part 1. Stationary helically coiled tubes. AIChE J. 21 : 965-974.

[16] Larrain,J. and Bonilla,C.F. (1970) Theoretical analysis of pressure drop in the laminar flow of fluid in a coiled pipe. Trans. Soc. Rheol.14 : 135-147.

[17] Le Tallec,P. (1980) A mixed finite element approximation of the Navier-Stokes equations. Numer. Math. 35 : 381-404.

[18] McConalogue,D.J. and Srivastava, R.S. (1968) Motion of fluid in a curved tube. Proc. R. Soc. London Ser.A. 307 : 37-53.

[19] Srivastava,R.S. (1980) On the motion of a fluid in a curved pipe of elliptical cross-section. Z. Angew. Math. Phys. 31 : 297-303.

[20] Taylor,C. and Hughes,T.G. (1981) Finite element programming of the Navier-Stokes equations. Pineridge Press.

[21] Temam,R. (1984) Navier-Stokes equations : Theory and numerical analysis. Studies in mathematics and its applications. Vol.2. North-Holland.

[22] Truesdell,L.C. and Adler,R.J. (1970) Numerical treatment of fully developed laminar flow in helically coiled tubes. AIChE J. 16 : 1010-1015.

[23] Wang,C.-Y. (1981) On the low-Reynolds-number flow in a helical pipe. J. Fluid Mech. 108 : 185-194.